FINAL REPORT

ON

A Proposed Triaxial Digital Fluxgate Magnetometer for NASA Applications Explorer Mission: A Design Study

NAS 5-23660

R.L. McPherron

A PROCEDURE FOR ACCURATE CALIBRATION OF THE ORIENTATION OF THE THREE SENSORS IN A VECTOR MAGNETOMETER

June 1977

Institute of Geophysics and
Planetary Physics
University of California
Los Angeles, California 90024

CONTENTS

PRECEDING PAGE BLANK NOT FILMED

INTRODUCTION

At a recent conference of the American Geophysical Union it was concluded that existing data are inadequate to provide definitive models of the earth's magnetic field (Cain, 1975). One of the main reasons is that complete spatial coverage of only the field magnitude at any instant of time is insufficient to uniquely define a vector field. This problem was first recognized by G. Backus and as discussed by Stern 1975, leads to large errors in certain terms of the spherical harmonic expansion of the earth's field.

As a consequence of the forgoing problem many investigators have suggested that a satellite survey of the vector magnetic field is required. The program proposed by NASA to accomplish this survey has been called MAGSAT. At the present time, several study contracts have been let by NASA to examine the feasibility of the proposed survey. These studies include three different topics; A stable boom design study, An attitude transfer design study, and A vector magnetometer design study.

This report is devoted to one aspect of the vector magnetometer design study, a procedure for calibration of the vector magnetometer. This report is number 3 in a series of three reports under preparation by the University of California in Los Angeles on contract #NAS 5-23660. The preceding reports McLeod, 1976, 1977, described a triaxial fluxgate magnetometer suitable for the proposed mission.

The body of this report is divided into three main sections. The first describes necessary preparations of the test facility. The second describes the calibration procedure for individual sensors. The third describes procedures for calibrating the sensor assembly.

SPECIFICATIONS OF THE VECTOR MAGNETOMETER

The specifications for the vector magnetometer described in RFP-566233/326 are included here as Appendix A1. These specifications may be summarized as follows. The design goal for the magnetometer is to measure three components of the magnetic field in sensor coordinates with a resolution of one gamma and an absolute accuracy better than five gamma in a $\pm$ 64,000 γ field. This is to be accomplished for at least one year over a broad range of sensor and electronics temperatures. The magnetometer must be constructed so that its accuracy is not impaired by extreme thermal shock and exposure to acceleration. The sensor offsets must be less than 0.4 γ and cannot drift more than this amount in one year. Noise in the sensor outputs must be less than 0.1 γ zero to peak in the bandwidth 0.1 to 25 Hertz. Magnetic axes of each sensor must be orthogonal within 0.1 degree, known to one arc second and stable to five arc seconds.

COMMENTS ON SPECIFICATIONS

As pointed out by the author in his proposal for this design study, these specifications far exceed those of any magnetometer previously carried by satellite and in fact exceed those of most ground magnetic observatories. The only detailed report of an observatory which meets these specifications is by Yanagihara, et al., 1973, describing the Kakioka observatory in Japan. It should be noted that this observatory has a staff of nearly 50; its instruments are on fixed granite pillars in temperature controlled rooms; calibrations of all instruments are carried out on an almost daily basis.

The author believes that most of the magnetometer specifications can be met by careful electronic and mechanical design. The most serious problem

however, is angular calibration and stability of the sensors. For example, according to Yanagihara et al., 1973, ordinary magnetic theodolites can determine the direction of an unknown field to no better than 6 arc seconds. A specially built theodolite in use at Kakioka (A-56, universal standard magnetometer) could only obtain 3 arc second accuracy. A more recent version of this instrument, the DI-72 has obtained an accuracy of one arc second.

It goes without saying that the accuracy of a calibration can be no better than that of the test facility. Thus, from the preceding discussions it would appear that the calibration of the orientation of the test coil will be limited to about 6" unless special equipment is available. This in turn would impose a similar error on the magnetometer calibration.

In this report we develop an alternative procedure for angular calibration that does not require a magnetic theodolite. Instead, we use measurements made by the sensor under calibration to simultaneously determine the orientation of both the test coil and sensor. As we will show, this procedure is limited by the accuracy with which the magnitude of the calibration field can be measured and by the accuracy of the sensor's sensitivity and offset.

DESCRIPTION OF TEST FACILITY

To meet the specifications of Appendix A1 it will be necessary to carry out the magnetometer calibration in a well calibrated magnetic test facility. At the present time there are only two such facilities in the U.S., one at Goddard Space Flight Center and one at the Ames Research Laboratory. The Ames facility has a rather small set of calibration

coils and no provisions for thermal-vacuum calibration, consequently, we will assume that the test will be carried out at GSFC.

A brief summary of some of the facilities available at GSFC for magnetometer testing is given in a report by C.A. Harris, 1971. The magnetic field component test facility consists of a 22 foot diameter three component coil system with remotely isolated magnetometer and control instrumentation buildings. The orthogonal field cancelling coils are sufficiently large that nearly any magnetic field may be produced in a sphere of diameter 3 feet. The main winding of each coil is connected to one axis of a 3 axis resonance magnetometer which senses the variations in the earth's field and feeds back a current which cancels this field. The main winding is also connected to a D.C. field generator which can produce fields of up to 60,000γ in 0.1γ steps. A second winding on each coil is used to cancel the temperature dependence of the main winding. A third winding is used to mimimize field gradients over the test volume.

The orthogonal coils are oriented with X horizontal towards magnetic north, Y horizontal to the east, and Z vertically downward. The field generators can produce 60,000γ in Z, 25,000γ in X and 6,000γ in the east-west direction. Accuracy of field nulling is of order 0.2γ. The gradients across the 3 foot test volume are such that the field does not depart from the center value by more than 0.6γ.

DESCRIPTION OF TEST EQUIPMENT

Several pieces of test equipment of high precision and accuracy are required to carry out the calibrations of the test facility and magnetometer.

In this report we assume the following items are available.

1) 6 digit - digital voltmeter
2) 3 precision resistors
3) Proton precession magnetometer
4) 2- 3 component station magnetometers
5) 2 - Optical theodolites (autocollimaters)
6) 2 - Precision levels
7) Optical octagon
8) Brass fixture for rotating sensor assembly
9) Programmable digital data logging system with analog and digital inputs as well as keyboard entry

Calibration of Test Facility

To accomplish the absolute accuracy required by the mission requirements it is necessary to calibrate the test facility first. Steps in this procedure are described in the following subsections.

Measure Calibration Coil Constants

Place a precision resistor in the current loop from the DC field generator to the main winding of each coil. Monitor the voltage drop across the resistor with the digital voltmeter. Fix the proton precession magnetometer at the center of the test volume. Increment the field generator in 5000 steps across the full range of the proton precession magnetometer ($\approx$ 20,000-60,000γ). For each step record the field measured by the proton magnetometer 10 times and average. Also record the reading of the digital voltmeter and convert to current using the known resistance. Repeat for the same range of negative field values.

Fit a straight line to the field versus current data determining the coil constant (slope) and coil offset (intercept). $B = kI + B_o$. Also determine the probable errors in these constants using the known accuracy of the precision resistor and digital voltmeter as well as the standard deviation of the proton magnetometer measurements. Assign a probable error to any test field calculated on a basis of this formula.

If the coil offset is not zero or there are systematic departures of the field from the linear relationship then a more elaborate calibration will be required. This possibility exists since the calibration field generator output is mixed with the output of the resonance magnetometer which nulls the earth's field.

Minimize Calibration Coil Gradients

Set the maximum possible field in a coil. Use the proton precession magnetometer to measure the field along the coil axis at 6 inch intervals. Fix the magnetometer at the point of maximum deviation from the center value. Alter the current in the gradient adjustment coils to reduce this deviation as much as possible. Repeat the survey along the coil axis. Again, fix the magnetometer at point of maximum deviation and again adjust. Iterate this procedure until the field is as uniform as possible.

Test Earth Field Nulling System

The earth's field nulling system is a servo loop with the sensors physically separated from the region in which the field is being nulled. Inevitably there are small differences in field between these two locations which the sensors cannot measure. Because of this there will be a small,

residual field at the center of the coil system. This field will have both constant and time varying components. The magnitude of these components limits the accuracy of any magnetometer calibrations. The residual field can be measured in the following manner.

Place a calibrated three component fluxgate magnetometer at the center of the coil system. Align the sensors roughly along the coil axis. Record the output of this magnetometer with the digital data acquisition system.

Perform three series of measurements. First, record about 1 minute of data at a sample rate exceeding 120 samples per second. Next record one hour of data at a sample rate of 2 samples per second. Finally record 8 hours of data at a sample rate of one sample per 5 seconds. Repeat this series of measurements for the following conditions: Midweek workday, midweek night shift, weekend midday, weekend night shift.

The data gathered in the foregoing experiments should then be subjected to power spectral analysis. For each set of conditions separate auto spectra are calculated for data at each sample rate. These auto spectra can then be plotted as log power versus log frequency on the same graph. The data define the magnetic noise in the test facility from about 0.3 millihertz to 100 Hertz. A separate graph for each set of conditions show how this noise is a function of time during the work week.

To define the expected error in any particular magnetic field measurement we integrate under the appropriate noise spectrum. For a lower frequency limit use the reciprocal of the duration of the measurement (the time during which we must assume the field is constant). For an upper limit use the Nyquist frequency of the magnetometer making the field measurement. The rms field error is the square root of the area under the noise power curve between the specified limits.

Definition of Geographic Coordinates

Test procedures described below require the definition of an accurate geographic coordinate system. This can be done as described below.

A test table is installed in the center of the coil system with its surface about six inches below the center line of the horizontal coils. The table should be made of either granite, marble or glass. It must be nonmagnetic and rigidly attached to pylons sunk to bedrock. It should have provision for adjusting the surface using precision levels to be exactly level. The table should also provide a means for rigidly attaching a straight edge to the surface of the table. (This is used where repetitive measurements with 180° rotation are required.)

Once the test table is installed and leveled the geographic coordinate system is established with the use of two theodolites as shown in figure 1. The first theodolite is placed north of the test table on a strut or pylon sunk to bedrock. This should not be one of the fixtures holding the calibration coils. Later it will be important to determine the orientation of the coil axis in geographic coordinates. This can not be done if the theodolites are attached to the coil supports.

The theodolite is leveled by placing a mirror on the test table at the exact center of the test coils. The mirror is gradually rotated (with tangent screws) until the reflected beam is observed in the theodolite. The theodolite is translated vertically and horizontally until it is level with the telescope in the same plane as the mirror.

A second theodolite is placed at the same distance as the first but to the east of the coil center. The mirror is replaced by a right angle reflector. The second theodolite is translated until a beam from the first enters the second theodolite when it is exactly level.

The geographic coordinate system defined in this manner has the X and Y axes in the horizontal plane. The X axis is roughly aligned with the north coil axis and the Y axis with the east coil axis. The Z axis is vertically downward and can be defined by levels when necessary.

The magnetic field in geographic coordinates can be written as a vector sum

$$\underset{\sim}{B}(GEO) = B_X \hat{n}_X + B_Y \hat{n}_Y + B_Z \hat{n}_Z \tag{1}$$

In this formula B_i is the magnetic field produced by the i^{th} test coil and given by the relation

$$B_i = k_i I_i$$

where I_i is the current and k_i the coil constant for the i^{th} coil. Also, $\hat{n}_i$ is a unit vector parallel to the magnetic axis of the i^{th}coil. In geographic coordinates we may write $\hat{n}_i$ as a column vector

$$\hat{n}_i = (n_{Xi} \hat{X} + n_{Yi} \hat{Y} + n_{Zi} \hat{Z}) \tag{2}$$

where $\hat{X}$, $\hat{Y}$, $\hat{Z}$ are the orthogonal unit vectors of geographic coordinates defined by the theodolites and the vertical direction. Substituting for $\hat{n}_i$ in equation (1) we find

$$\begin{aligned}\underset{\sim}{B}(GEO) = {} & (n_{XX} B_X + n_{XY} B_Y + n_{XZ} B_Z) \hat{X} \\ & + (n_{YX} B_X + n_{YY} B_Y + n_{YZ} B_Z) \hat{Y} \\ & + (n_{ZX} B_X + n_{ZY} B_Y + n_{ZZ} B_Z) \hat{Z}\end{aligned}$$

This may be written as

$$\underset{\sim}{B}(GEO) = (n) \underset{\sim}{B}(COIL) \tag{3}$$

Here $\underset{\sim}{B}(COIL)$ is a vector with components made up of the fields generated by each coil. The matrix (n) has columns made up of the unit vectors $\hat{n}_X$, $\hat{n}_Y$, $\hat{n}_Z$.

Definition of Sensor Coordinates

A second coordinate system fixed with respect to the magnetometer sensors must also be defined. In our procedures this system is defined by an optical polygon rigidly attached to the orthogonal array of sensors. For reasons discussed later this should be an octagon with all sides and top face silvered. The octagon is glued to the sensor assembly with one face as nearly perpendicular to the X sensor axis as possible. Also the top of the polygon is aligned with its face as nearly normal to the axis of the Z sensor as possible.

For purposes of discussions we assume the sensor assembly consists of a cube approximately 3 inches on a side (typical ring core fluxgate array). In this case, the polygon might be mounted on top of the assembly and appear as shown schematically in Figure 2.

With Sensor Coordinates defined as above the X sensor is approximately aligned with the X axis of sensor coordinates and similarly the Y and Z sensors are nearly aligned with Y and Z coordinate axes.

In sensor coordinates we can write the magnetic field measured by the i^{th} sensor as

$$M_j = \underset{\sim}{B} \cdot \hat{m}_j \qquad j = 1, 2, 3 \qquad (4)$$

where $\underset{\sim}{B} = \underset{\sim}{B}$(SEN is the actual magnetic field and $\hat{m}_j$ is unit vector along the j^{th} sensor axis, both in Cartesian sensor coordinates. If we write $\hat{m}_j$ as a column vector we have

$$\hat{m}_j = m_{xj}\,\hat{x} + m_{yj}\,\hat{y} + m_{zj}\,\hat{z} \qquad (5)$$

where $m_{ij} = \hat{x}_i \cdot \hat{m}_j$ is the direction cosine of the unit vector $\hat{m}_j$ with respect to the i^{th} axis of sensor coordinates. Similarly, we write

$$\underset{\sim}{B} = B_x\,\hat{x} + B_y\,\hat{y} + B_z\,\hat{z}$$

Substituting in equations (4) we obtain

$$M_x = m_{xx} B_x + m_{yx} B_y + m_{zx} B_z$$

$$M_y = m_{xy} B_x + m_{yy} B_y + m_{zy} B_z$$

$$M_z = m_{xz} B_x + m_{yz} B_y + m_{zz} B_z$$

This may be written in matrix form as

$$\underline{M} = (\mu^T)\ \underline{B}(SEN) \qquad (6)$$

The matrix (μ) is a matric whose columns are the unit vectors along the magnetic axes of the three sensors. The vector $\underline{M}$ is a vector with components given by the actual measurements made by the three sensors. The inverse of eq. (6) allows one to obtain a Cartesian vector from the actual measurements, i.e.

$$\underline{B}(SEN) = (\mu^T)^{-1}\ \underline{M} \qquad (6A)$$

It should be noted that the vector $\underline{M}$ is not the representation of the actual magnetic field in a non-Cartesian coordinate system aligned with the sensor axes. If we want this representation we must write

$$\underline{B} = B_z' \hat{m}_x + B_y' \hat{m}_y + B_z \hat{m}_z$$

$$= B_x' [m_{xx} \hat{x} + m_{yx} \hat{y} + m_{zx} \hat{z}]$$

$$= B_y' [m_{xy} \hat{x} + m_{yy} \hat{y} + m_{zy} \hat{z}]$$

$$= B_z' [m_{xz} \hat{x} + m_{yz} \hat{y} + m_{zz} \hat{z}]$$

Rearranging terms this becomes

$$\underline{B}(SEN) = \mu\ \underline{B}(MEA)$$

where $\underline{B}(MEA) = (B_x', B_y', B_z')$ is the representation of $\underline{B}$ in the non-Cartesian coordinate system aligned with the magnetic axes of the sensors. Using the result, eq. (6) we find

$$\underline{M} = (\mu^T \mu)\, \underline{B}(MEA)$$

or finally

$$\underline{B}(MEA) = (\mu^T \mu)^{-1}\, \underline{M}$$

Preparation of Magnetometer Test Fixture

The test procedures discussed below require that the sensor assembly be oriented in a variety, of precisely known orientations relative to geographic coordinates. This is accomplished by rigidly attaching an optical polygon to the sensor assembly. Reflections from the faces of these polygons are monitored by the two theodolites and used to calculate the precise orientation of the polygon. The difficulty with this procedure is the limited field of view of the theodolites. It is not possible to perform arbitrary reorientations of the sensor assembly and have a face of the polygon nearly normal (within about a half degree) of the theodolite optical axis.

To solve the foregoing problem we utilize a magnetometer test fixture which makes possible reasonably accurate rotations about two orthogonal axes. An example of such a fixture is shown in Figure 3. The device shown is an earth inductor or magnetic theodolite. Its purpose is the accurate determination of the direction of an unknown magnetic field. It utilizes a spinning search coil to indicate when the search coil

rotation axis is aligned with the ambient field. The azimuth and elevation of the rotation axis are read from horizontal and vertical circles.

We propose to modify such a device as shown schematically in figure 4 The search coil drive assembly is replaced by hollow tubes concentric with the elevation axel (horizontal axis). This allows unobstructed observation of one face of the optical octagon when mounted within the fixture. The search coil is replaced by a mounting plate with attachment clamps. The platform and clamps are provided with adjustments which enable the experimentor to align the optical axes of the polygon with the rotation axes of the fixture.

The procedure for setting up such a fixture would be as described below. Place the magnetometer sensor assembly on the mounting plate of the fixture. The plate should be designed such that the center of the optical polygon is close to the intersection of the vertical and horizontal axes of the fixture. Place the fixture on the test table with the horizontal axis pointing north and the center of one face of the octagon in line with the north theodolite. Move the fixture along the north-south line until the center of an orthogonal face is roughly aligned with the east theodolite. Level the fixture using the three leveling screws and levels attached to the base of the fixture. Rotate the fixture in azimuth with a tangent screw until the normal to the northward face lies in a vertical plane passing through the north theodolite. Next, use the adjustment screws on the mounting plate to bring the normal to the east face into a vertical plane passing through the east theodolite. Repeat these steps until both faces of the polygon are nearly orthogonal to the two theodolites. When this is achieved the top surface of the polygon should be almost level.

Now continue with fine adjustment of fixture level to bring the azimuth axel (vertical axis) vertical. Do this by rotating in azimuth by 45° increments. If the successive faces do not produce centered images in the theodolites the azimuth rotation axis is not truly vertical. Make it so by fine adjustments of fixture level.

When the foregoing procedure is completed it should be possible to perform rotations through angles of integral multiples of 45° and maintain reflected images of crosshairs within the field of view of the theodolites. Because of the inaccuracies associated with the bearings of the test fixture it is not expected that the rotation axis will be stable to much better than some fraction of a minute of arc. Also errors associated with the verniers on the azimuth and elevation circles will limit the accuracy of rotation angles to some fraction of a minute.

This problem is not important. Actual alignment of the sensor coordinates in geographic coordinates is determined by the theodolite reflections from the precisely constructed faces of the optical octagon. The primary purpose of the fixture is to provide sufficiently accurate rotations that the reflected images remain within the field of view of the theodolites.

Relation between Sensor and Geographic Coordinates

In the previous section we described a procedure for setting up a test fixture which holds the array of sensors to be calibrated. The sensor assembly has attached to it an optical octagon with its top and side faces silvered. The faces of this octagon must be constructed so that they meet at 45° angle and are flat to better than one arc second. The top must be at 90° to all faces within the same accuracy. The fixture

is sufficiently precise that it can rotate the sensor assembly through angles in increments of 45° so that images reflected to the theodolites viewing the orthogonal faces of the octagon remain in the field of view. It is not expected that these images will be exactly centered. The exact orientation is thus determined by using the theodolites as autocollimators reading the precise orientation to a fraction of an arc second.

As an example, consider the case shown in the top of Figure 5 for which the X and Y axes of sensor and geographic coordinates are approximately aligned. In actual fact, the X axes are not exactly coincident as shown in the lower left. The azimuthal angle ϕ_X between the X axes in the horizontal plane is measured by the horizontal displacement of the image in the north theodolite. Similarly the polar angle θ_X is given by the vertical displacement of the image in this theodolite. Using these angles we can express the direction cosines of the $\hat{X}$ axis of sensor coordinates in geographic coordinates as

$$\hat{X}_S(GEO) = [\cos\phi_X \sin\theta_X,\ \sin\phi_X \sin\theta_X,\ \cos\theta_X] \tag{7}$$

Similar measurements made with the east theodolite give the $\hat{Y}$ axis as

$$\hat{Y}_S(GEO) = [\cos(\phi_Y+90)\ \sin\theta_Y,\ \sin(\phi_Y+90)\ \sin\theta_Y, \cos\theta_Y] \tag{8}$$

Finally the direction cosines of the $\hat{Z}$ axis are found by the requirement that $\hat{Z}_S$ is orthogonal to $\hat{X}_S$ and $\hat{Y}_S$.

$$\hat{Z}_S(GEO) = \hat{X}_S \times \hat{Y}_S \tag{9}$$

Where $\hat{X}_S$ and $\hat{Y}_S$ are given as above.

The transformation from geographic to sensor coordinates is found by using the rule that the rows of the transformation matrix are the unit vectors of the new coordinate system expressed in the old system. Thus

$$\underset{\sim}{B}(SEN) = (R)\ \underset{\sim}{B}(GEO) \tag{10}$$

where

$$(R) = \begin{pmatrix} X_X & X_Y & X_Z \\ Y_X & Y_Y & Y_Z \\ Z_X & Z_Y & Z_Z \end{pmatrix} \tag{11}$$

Successive rows of (R) are given by the elements of the vectors appearing in equations 7, 8, and 9 respectively.

With the results presented above and in previous sections we can easily relate the measured magnetic field to the field produced by the test substituting equation (3) into (10) we have

$$\underset{\sim}{B}(SEN) = (R)(\eta)(BCOIL)$$

then, substituting this result in equation (6) we find

$$\underset{\sim}{M} = (\mu^T)(R)(\eta)\underset{\sim}{B}(COIL) \tag{12}$$

Equation (12) graphically illustrates the fact that any measurement made in the calibration facility couples the unknown direction cosines of both the coil and the magnetometer axes. Also it is apparent that this equation is nonlinear in the unknowns. If we perform a number of experiments creating a set of such equations we must solve a set of simultaneous, nonlinear equations. This problem is further complicated by the fact that each column of (μ) and (η) is a unit vector, i.e. there are only 2 unknowns rather than three per column. Thus, altogether there are 12 unknowns to be determined experimentally. A procedure for accomplishing this is described in a subsequent section.

CALIBRATION OF INDIVIDUAL SENSORS

The second major step of the vector magnetometer calibration procedure is the calibration of individual sensors. This calibration includes the determination of sensor sensitivity offset, noise and drift. In addition, it involves the measurement of the effects of temperature and magnetic fields orthogonal to the sensor. In following subsections we discuss each of these procedures in detail.

Measurement of Sensor Sensitivity and Nonlinearity

The component of magnetic field parallel to the axis of a linear fluxgate sensor may be written

$$B_i = k_i V_i + O_i \tag{13}$$

In this equation V_i is the sensor sensitivity in gamma/volt, and O_i is the sensor offset in gamma. To determine these constants we must apply known magnetic fields B and measure the sensor output voltage, $V_i(B_v)$. Plotting the applied field as a function of output voltage, the slope of a best fit straight line determines the sensitivity and the intercept determines the offset, O_i. Systematic deviations of the measurements from the best fit line indicate that the sensor is not truly linear.

Normally, the sensitivity of a magnetometer is determined from only two sets of measurements, one at zero field and one near full range. In the following paragraphs we show this procedure is not sufficiently accurate to meet the requirement of 1 gamma absolute accuracy over the full dynamic range of the sensor. Consequently, it is necessary to make a large number of measurements across the full dynamic range of the sensor. These measurements are then fit by a least square straight line. This

procedure improves the accuracy of the sensitivity determination and has the additional advantage that a plot may be made of the deviation of the observations from the best fit.

To estimate the accuracy of a particular magnetic field measurement based on equation (13) we note

$$\delta B = \delta(k\ V) + \delta(0)$$

but

$$\frac{\delta(k\ V)}{kV} = \left[\frac{\delta k}{k} + \frac{\delta V}{V}\right]$$

$$\delta B = kV\left[\frac{\delta k}{k} + \frac{\delta V}{V}\right] + \delta(0) \tag{16}$$

A crude estimate of the values of k and 0 and their errors can be made by using only two sets of measurements. Suppose B_0 and V_0 correspond to zero field and B_1 and V_1 correspond to 50,000$ and 10 volts. Then, from equation (13)

$$k = \frac{B_1 - B_0}{V_1 - V_0} \quad \text{and} \quad 0 = \frac{V_1 B_0 - V_0 B_1}{V_1 - V_0} \tag{17}$$

We can show

$$\frac{\delta k}{k} = 2\frac{\delta B}{B_1} + 2\frac{\delta V}{V_1} \tag{18}$$

and

$$\frac{\delta 0}{0} \cong \left[\frac{\delta B}{B_1} + \frac{\delta V}{V_1}\right] B_1 + \left(\frac{\delta V}{V_1}\right) 0 \tag{19}$$

Since $B_1 >> 0$ we have finally

$$\frac{\delta B}{B} \cong kV\left[2\frac{\delta B}{B_1} + 3\frac{\delta V}{V_1}\right] + \left[\frac{\delta B}{B_1} + \frac{\delta V}{V_1}\right] B_1 \tag{20}$$

For a voltage V close to V_1, $kV \approx B_1$ so that

$$\frac{\delta B}{B} \sim 3\frac{\delta B}{B_1} + 4\frac{\delta V}{V_1} \tag{21}$$

For most test facilities it is difficult if not impossible, to generate a calibration field accurate to better than 1γ in 50,000γ. Also available digital voltmeters can measure to an absolute accuracy of about 50μ V in 10 volts. Thus we take

$$\delta B/B = 1\gamma/50{,}000\gamma = 20 \times 10^{-6}$$
$$\delta V/V = 50 \times 10^{-6}/10 = 5 \times 10^{-6}$$

It is evident that the accuracy of the calibration field is most important in determining the final accuracy of the calibrated sensor. Substituting in equation (21) we find for full range

$$(\delta B/B)_{max} = 80 \times 10^{-6} \quad \text{or} \quad \delta B_{max} \simeq \pm 4\gamma$$

The minimum error occurs for zero field and depends on the error in the offset

$$(\delta B)_{min} = \delta 0 \cong [\delta B/B_1 + \delta V/V_1]\, B_1$$

Numerically

$$(\delta B)_{min} \simeq 1.25\gamma$$

These errors are unacceptably large and demonstrate the need for a more accurate calibration procedure. In the following subsection we describe an independent procedure for determining offset to an accuracy of $\simeq$0.1γ. Next, however, we consider the improvement in accuracy obtained by the least square procedure mentioned above.

In fitting a straight line to the calibration date we write

$$B_\nu = A_0 + A_1 V_\nu \qquad \nu = 0, 1, 2, \ldots N$$

Here ν is in index referencing one of the pairs of N+1 calibration measurements. In this procedure we choose V_ν as the dependent variable, because it can be measured more accurately than B_ν. In the usual least square error

analysis it is assumed that the dependent variable is error free. Using results derived in Hildebrand, 1956, we can show the coefficients A_k satisfy the set of normal equations

$$(c)\ \underset{\sim}{A} = \underset{\sim}{V} \tag{23}$$

where

$$\underset{\sim}{A} = \begin{pmatrix} A \\ A_1 o \end{pmatrix}$$

$$\underset{\sim}{V} = \begin{pmatrix} \sum_{i=0}^{N} B_i \\ \sum_{i=0}^{N} V_i B_i \end{pmatrix}$$

$$c = \begin{pmatrix} (N+1) & \sum_{i=0}^{N} V_i \\ \sum_{i=0}^{N} V_i & \sum_{i=0}^{N} V_i^2 \end{pmatrix}$$

The error in each coefficient δA_k is given by

$$\delta A_k^2 = (c^{-1})_{kk} \left(\frac{N+1}{N-1}\right) \varepsilon_{RMS}^2 \tag{24}$$

where

$$\varepsilon_{RMS}^2 = \frac{1}{N+1} \sum_{i=0}^{N} (\hat{B}_i - B_i)^2$$

Note ε_{RMS}^2 is the mean square deviation of the observations from the predictions; i.e. δB in our previous discussion.

The normal matrix c is easily inverted so that

$$(c^{-1}) = \frac{1}{|c|} \begin{pmatrix} \sum_i V_i^2 & -\sum_i V_i \\ -\sum_i V_i & (N+1) \end{pmatrix}$$

and

$$|c| = (N+1) \sum_{i=0}^{N} V_i^2 - \left(\sum_{i=0}^{N} V_i\right)^2$$

To estimate the errors we must assume some model of the calibration procedure.

Therefore, assume 10 volts corresponds to 50,000Ω and that we step through the dynamic range 0 - 50,000Ω in 500Ω steps, i.e. 100 steps of 0.1 volt. Then (N+1) = 101

$$\sum_{i=0}^{N} V_i = .1 \sum_{i=0}^{100} (i) = .1[\tfrac{1}{2}(100)(101)] = 505$$

$$\sum_{i=0}^{N} V_i^2 = (.1)^2 \sum_{i=0}^{100} (i)^2 = .01[338,350] = 3383.50$$

Thus $|c| = (101)(3383.50) - (505)^2 = 86,708.5$

Hence, $(c^{-1})_{00} = \dfrac{\Sigma_i V_i^2}{|c|} = .03902$

$$(c^{-1})_{11} = \frac{N+1}{|c|} = .0011648$$

For N = 100 we have

$$\delta A_k \cong \sqrt{(c^{-1})_{kk}}\, \varepsilon_{RMS}$$

Thus

$$\delta A_0 \approx .2\, \varepsilon_{RMS}$$
$$\delta A_1 \approx .034\, \varepsilon_{RMS} \qquad (25)$$

This result should be compared to our previous error estimates based on two pairs of measurements. Using equations (18) and (19) and ignoring δV we found

$$\delta A_0 = \delta 0 \approx \delta B = 1.0\, \varepsilon_{RMS}$$
$$\delta A_1 = \delta k \approx \frac{2k}{B_{11}}\, \delta B = \frac{2B_1}{V_1} \frac{\delta B}{B_1} = \frac{2}{V_1}\, \delta B = .2\, \varepsilon_{RMS}$$

The use of 100 pairs of measurements should improve the calibration by about a factor of 5.

The error in a field measurement was according to equation (16),

$$\delta B = kV \left[\frac{\delta k}{k} + \frac{\delta V}{V}\right] + \delta 0$$

since $\delta A_0 = \delta 0$ and $\delta k = \delta A_1$ we have

$$\delta B_{max} = 5 \times 10^4 \left[6.8 \times 10^{-6} \varepsilon_{RMS} + 5 \times 10^{-6}\right] + .2\, \varepsilon_{RMS}$$

If $\varepsilon_{RMS} = 1\gamma$,

$$\delta B_{max} \sim .6 + .2 = .8\gamma$$

While the foregoing error is quite acceptable it depends on the linearity of the magnetometer. If the observations systematically depart from a straight line ε_{RMS} will be larger than 1γ, and δB_{max} will be proportionally larger. In this case, it might be necessary to use higher order functions to fit the observations.

On a basis of the preceding analysis we recommend the procedure shown schematically in figure 6, to determine sensitivity and offset of each sensor. Attach the sensor to a test fixture which has provisions for slight rotations of the sensor about two axes. Place the fixture on the test table with one edge against a north-south straight edge attached to the table. Apply maximum field ($\approx$50,000γ) in the north direction. Rotate the sensor around a vertical axis to obtain maximum output voltage. Next, rotate the sensor about a horizontal axis again maximizing the output voltage. Repeat these steps several times until the best possible alignment of sensor magnetic axis and calibration field is obtained.

Once alignment is achieved perform a sequence of measurements determining sensor output voltage as a function of calibration magnetic field. To determine the precise input field use a digital voltmeter to monitor the voltage drop across a precision resistor placed in the field generation drive circuit. Using the calibration coil constant determined

by the method described above and the measured coil current (I_{COIL} = V/R) calculate the applied field. Also use the digital voltmeter to measure the sensor output voltage corresponding to the input field.

To obtain sufficient accuracy perform 101 pairs of measurements with the input field incremented in 1000 steps over the range -50,000 to +50,000γ. Enter the table of measurements, B_i versus V_i into a computer program which fits a least square line to the data determining k, 0 and their associated errors. The program should also calculate and plot the deviation of the predicted field from the observed field. If the resulting time series is Gaussian with zero mean the sensor is linear.

This procedure is repeated twice more for the remaining two sensors. Together these three experiments define the sensitivities and offsets required to measure the three components of the magnetic field provided the orientation of each sensor is known in inertial space.

Measurement of Sensor Offset in Low Field

An independent, and more sensitive determination of sensor offset can be made by tests performed in a low field environment. This procedure is somewhat easier than the one described in the preceding subsection and because it does not require a large test facility, we recommend that it be used for long term monitoring of temporal drifts in offset.

The sensor offset is defined by equation (13)

$$B = kV + 0$$

Solving for the magnetometer output voltage we find

$$V = \frac{B-0}{k}$$

Suppose we place the sensor in alignment with a weak field B_0, the sensor output will be

$$V_1 = \frac{B_0-0}{k}$$

Now reverse the direction of the field either by a 180 rotation of the sensor or by changing the sense of the current producing the field. The output voltage is

$$V_2 = \frac{-B_0-0}{k}$$

Adding the two measurements and solving for 0 we have

$$0 = \left(\frac{V_1+V_2}{2k}\right) \qquad (26)$$

Note the sensitivity must be independently determined to calculate offset. The error in 0 is roughly

$$\delta 0 = \left[\frac{2\delta V}{V} + \frac{\delta k}{k}\right] 0$$

from equation (25) $\delta k/k \simeq 7 \times 10^{-6}$. However $\delta V/V$ is of order 1. The difference is that δV should not be the precision of the measurement device, but the fluctuation induced by variations in the ambient field and by

instrument noise. In an unshielded, industrial environment fluctuations in voltage δV correspond to field fluctuating of order 1γ. Since ring core offsets are of the same magnitude we expect $\delta V \sim V$. Clearly accuracy can be obtained only by repeated measurements in a shielded environment.

To carry out a determination of offset we recommend the following. Place the sensor on a fixture which allows an approximate 180° rotation. (An accuracy of a few degrees in this rotation is sufficient.) Place the sensor and fixture inside a set of concentric mu metal cans. Cover each can with its mu metal cap excluding the earth's field from the interior of the innermost can. A remanent magnetic field of a few gamma magnitude and unknown direction will remain in the can. Since the direction of this field cannot be changed the orientations of the sensor must be reversed. Perform a series of measurements of the magnetometer output voltage, rotating the sensor 180° before each measurement. Proceeding through the table of measurements, average pairs of readings and calculate offset. Average the offsets so determined to obtain a final, more accurate value.

Measurement of Sensor Noise in Low Field

In preceding sections we have discussed offset as if it were a constant property of the sensor. In fact, offset usually changes with time in a random manner. For fluxgate sensors, a frequency spectrum of these changes is typically inversely proportional to frequency. Thus, on a short time scale, variations in offset are quite small. In general, these variations are divided into two catagories depending on their time scale. Variations which take longer than some reference time are called offset while those that take less time are called noise. A typical reference time is between a day and a week.

Sensor noise is best characterized by a power spectrum of the sensor output when located in a zero field environment. In such a situation it can be assumed that all variations in output are a result of the instrument rather than the ambient field.

We suppose that the sensor has been placed inside a set of concentric mu metal cans as described in the previous subsection. The sensor output is recorded by a digital data acquisition system. Usually, it is necessary to amplify the magnetometer output voltage prior to digitization or quantization noise created by digitization will dominate the spectrum at higher frequencies. Also it is important to low pass filter the sensor output voltage with a time constant twice the sampling interval. This eliminates the problem of aliasing noise power from high to low frequencies in the digitization procedure.

Between 1000 and 5000 samples of the sensor output should be taken and then read into a computer program for spectral analysis. This program estimates the noise power in a frequency band corresponding to about 10/T to $1/2\Delta t$ where T is the duration of the series of measurements and Δt the sampling interval. For 5000 samples we have a ratio of upper to lower frequency limits of 250 or 2.4 decades of frequency.

To cover a wider band of frequencies in an efficient manner, we must repeat the above experiment with progressively higher sampling rates. A convenient set of experiments is summarized schematically in Figure 7. The frequency band from 10^{-4} Hertz (1 day) to 50 Hertz (100 samples per second) can be covered in three experiments. These are one day of recording with one minute samples, one hour of recording with one second samples and one minute of recording with 100 samples per second.

In order to consider the effects of quantization noise in this measurement we must assume some typical noise spectrum. For reference in

Figure 7 we have plotted a spectrum obtained at UCLA of a ring core fluxgate sensor scaled to ± 8000γ. Measurements made with ring core sensors scaled to ± 64,000γ are not significantly larger. For the curve shown the rms noise power over any three decades of frequency is 26×10^{-3}γ,

Quantization noise has a flat (white) spectrum with magnitude

$$P_Q(f) = \frac{(\delta B)^2}{12\, f_B}$$

where δB is the quantization level of the input data and f_B in the bandwidth of the measurements. Using the Nyquist frequency as the bandwidth we obtain

$$P_Q(f) = \frac{(\delta B)^2\, \Delta t}{6} \qquad (27)$$

According to this formula δB must satisfy

$$\delta B = \sqrt{\frac{6\, P_Q}{\Delta t}}$$

If we wish the quantization noise to be below the expected instrument noise in each experiment (see dashed lines in Figure 7) then we must have δB ... γ. For an instrument scaled to ± 50,000 this corresponds to

$$\delta B/B = 2 \times 10^{-7}$$

or 1 part in 5 million. Equivalently this is about $1/2^{22}$.

If we suppose instead the quantization corresponds to 1 gamma, then $P_Q = \Delta t/6$. This is plotted as a dashed line for the experiment Δt = .01 sec. Quantization noise is then several orders of magnitude greater than expected sensor noise.

From the foregoing discussion it is apparent that the magnetometer signal must be quantized to about 1 part in 2^{22} if we are to observe instrument noise when the dynamic range is ± 64,000γ. If the sensor has only a digital output quantized to 1γ in ± 64,000γ, sensor noise cannot be measured. If the sensor has an analog output, its output signal must be amplified so that the least significant bit of the data acquisition system correspond to about .02γ.

For example, suppose, 50,000γ corresponds to 10 volts. Then .02γ = 4μ volts. If the data acquisition system provides a 16 bit converter over a range 0-10 volts, the least significant bit is $\simeq$150μ volts. An amplification of about 40 is required to measure the sensor noise.

Our recommended procedure for measuring the noise of the sensors is summarized as follows. Place the sensor in a shielded container. Low pass filter and sample the output signal. Record the samples on digital tape and subject the data to spectral analysis. Plot the results as log power versus log frequency. Three separate experiments should be performed. These correspond to one day of 60 second samples, one hour of one second samples and 1 minute of .01 samples. To be meaningful the effective quantization of the data should be about .02γ in 50,000γ or 1 part in 2^{22}.

Measurement of Temporal Drift in Sensor Offset

In the preceding section we pointed out that sensor offset is time varying. By definition, changes in offset on a time scale longer than a day are called temporal drift. The drift can only be measured by repeated measurements at widely separated times. Since it would be difficult to routinely carry out such measurements in a large test facility we recommend use of the low field offset determination procedure.

To determine the nature and magnitude of temporal drift proceed as follows. Once a week place a continuously operating three component magnetometer in the test fixture inside a shielded can. Carry out a series of 180° rotations and calculate offset. Repeat for the remaining two axes. Return the magnetometer to an isolated location where it continues to monitor the earth's field. Plot the three sensor offsets as a function of time for about one year. At the end of the year determine the mean offset and rms deviation about the mean.

Measurement of Temperature Dependence of Sensitivity and Offset

It is well established that the sensitivity as well as offset of fluxgate magnetometers is a function of temperature. Since the sensor electronics is separated from the sensor assembly, both the electronics temperature (T_E) and the sensor temperature (T_S) are significant variables. Taking this dependence into account we rewrite equation (13) as

$$B_i = k_i(T_E, T_S)\, V_i + O_i(T_E, T_S) \tag{28}$$

Considering the two parameters k and O as functions of T_E and T_S we make the crude assumption

$$P(T_E, T_S) = P(T_{Eo}, T_{So}) + a\Delta T_E + b\Delta T_S \tag{29}$$

In this expression P is either of the two parameters k or O. The subscript "o" designates the nominal operating temperature (assume room temperature) of the sensor and electronics. ΔT is then the deviation of either temperature from the nominal value. Finally, a and b are temperature coefficients for the parameter.

It should not be expected that equation (29) applies over the full range of operating temperatures for the magnetometer. Experience at UCLA has shown that sensitivity is often a quadratic function of both temperatures. However, because of the rather large temperature dependence of typical fluxgate sensors the MAGSAT magnetometer will certainly have thermal enclosures about both the sensor assembly and sensor electronics. Within this enclosure temperature variations should be so small that equation (29) will be an adequate approximation.

To determine the temperature dependence of k and O we proceed as follows. Place the sensor assembly at the center of a three axis calibration coil facility. Align the three axes of the sensors as closely as possible with the three coil axes. Place thermal enclosures about both

the electronics and the sensor assembly. Using hot and cold gases bring both enclosures to nominal operating temperatures. Allow sufficient time for both units to come to the temperature of their respective enclosures (approximately one half hour). Determine the sensor offsets and sensitivities for each axis by applying a sequence of calibration fields in the appropriate calibration coil. Use least square procedures to calculate k_i and 0_i. Keeping electronics temperature constant increase sensor temperature by 5°. Allow the sensor to come to thermal equilibrium. Again carry out a series of measurements determining k_i and 0_i. Next, increment sensor temperature by 10°, establish thermal equilibrium, and determine k_i and 0_i. Finally, increment another 15° and determine k_i and 0_i. (Note this sequence defines the parameters for ΔT_S = 0°, 5°, 15° 30°.) Now return to nominal sensor temperature decrementing temperature by the same amounts as it was previously incremented. Continue to negative temperature deviations using the same scheme (ΔT = -5°, -10°, -15°). Finally, return to nominal sensor temperature.

Plot the parameters k_i and 0_i as functions of T_S. Fit straight lines to the three points at ΔT_S = -5°, 0°, +5°. The slope of these lines are the coefficients b in equation (29). The zero intercepts are the values $P(T_{Eo}, T_{So})$.

The foregoing procedure is now repeated holding sensor temperature constant and varying electronics temperature. Again a plot is used to determine the coefficient a in equation (29).

There is a remote possibility that all three sensors might have extrema for k_i and 0_i at nearly the same temperature. If this were the case it would be desirable to choose these common temperatures as the nominal operating temperatures and repeat the measurement of a and b about these new temperatures. It should be sufficient to use only three temperatures,

i.e., ΔT = -5°, 0° and +5°. For these points the coefficients a and b will be smaller and the magnetometer sensitivity to temperature will be reduced.

Measurement of Orthogonal Field Effects on Sensitivity and Offset

In the idealized theory of the fluxgate magnetometer the sensor response is unaffected by fields orthogonal to the sensor axis. Some sensors, however, have experimentally shown changes in properties when the orthogonal field is very large (McLeod, personal communication, 1976). Proper calibration of the MAGSAT magnetometer should include a demonstration that sensor properties do not change as a function of orthogonal fields.

To determine the effect of a strong orthogonal field we repeat the determination of sensitivity and offset described earlier. In this case however, the measurements are taken with a constant 60,000γ field in two directions normal to the axis under calibration. Both sensitivity (k) and offset (O) are determined as before. If the values for k and O differ by more than the experimental error a more elaborate calibration is required. If this is the case, we recommend that k and O be repeatedly determined for different values of orthogonal field. A possible series of measurements would start at -60,000γ and proceed to +60,000γ in 20,000γ steps. A plot of k and O as a function of orthogonal field should be made. Note this must be done for both possible orientations of orthogonal field.

If the suggested effect exists it will hopefully be small. In such an event, it may be possible to make a linear approximation of the dependence of k and O on orthogonal field magnitude. Data would be corrected by using the zero field constants to calculate the fields orthogonal to the sensor. These fields would then be used to determine

correct values of k and 0 and then a second calculation of the ambient field would be made.

CALIBRATION OF SENSOR ASSEMBLY

In this section we consider the most complex aspect of calibrating a vector magnetometer; determining the direction cosines of the magnetic axis of each sensor in a geometric coordinate system fixed in the sensor array. In section we showed

$$\underline{B}(GEO) = (\eta)\ \underline{B}(COIL) \tag{3}$$

$$\underline{M} = (\mu^T)\ \underline{B}\ (SEN) \tag{6}$$

$$\underline{B}(SEN) = (R)\ \underline{B}(GEO) \tag{10}$$

where "(GEO)" indicates a vector in Cartesian geographic coordinates (fixed in earth); "(SEN)" indicates a vector in Cartesian sensor coordinates (fixed in sensor assembly); "(COIL)" indicates a vector constructed from the magnitudes of the three fields generated by three, nearly orthogonal calibration coils, and $\underline{M}$ is a vector constructed from the magnitudes of the three fields measured by three, nearly orthogonal sensors. The matrices (η), (μ), and (R) are transformation matrices constructed from unit vectors. Columns of (η) are unit vectors of the calibration coil in geographic coordinates; columns of (μ) are unit vectors of the magnetic axis in sensor coordinates; columns of (R) are the unit vectors of the geographic coordinate system in sensor coordinates. Only the matrix (R) is orthogonal (i.e. $R^T = R^{-1}$) since the sets of unit vectors M_i and η_k are not orthogonal, i.e.

$$\hat{m}_i \cdot \hat{m}_j \neq 0 \qquad \hat{n}_i \cdot \hat{n}_j \neq 0$$

In these expressions we assume that accurate determinations of the coil constants and sensor sensitivity and offset have been already performed as described in earlier sections.

The basic problem is to determine the direction cosines of the magnetic axes $\hat{m}_x$, $\hat{m}_y$, $\hat{m}_z$ in sensor coordinates. This must be done by generating known fields $\underline{B}$(COIL) and measuring the output $\underline{M}$. From

(3), (6) and (10) we have

$$\underline{M} = (\mu)^T \quad (R)\ (\eta)\ B(COIL) \tag{12}$$

The transformation (R) from geographic to sensor coordinates can be experimentally measured as described in previously. Also $\underline{M}$ and $\underline{B}(COIL)$ are known experimentally. Clearly, we cannot find the elements of (μ) unless we already know the elements of (η) or unless we determine them simultaneously. We discuss these two cases separately in following sections.

Determination of Magnetic Axes Orientation Given Direction Cosines of Coil System.

If (η) is known in eq. (12) as well as $\underline{B}(COIL)$ and $\underline{M}$ we have three equations and nine unknowns. If we perform two additional experiments using different calibration fields we will have nine equations and nine unknowns which enables us to solve for the elements of the matrix (μ).

The simplist sequence of calibration fields to use in this procedure is one in which successive calibration fields are parallel to the coil axes. We thus have the three vector equations

$$\underline{M}_j = [(\mu)^T\ (R)(\eta)]\ \underline{B}_i(COIL) \qquad i = 1,2,3$$

where $$B_i(COIL) = \begin{pmatrix} \delta_{1i} \\ \delta_{2i} \\ \delta_{3i} \end{pmatrix} B_i(COIL) \qquad \delta_{ij} = 0 \quad i \neq j \qquad = 1 \quad i=j$$

We assume for convenience that the geographic and sensor coordinate systems have been constructed such that their axes are nearly aligned with those of the calibration coils and magnetic sensors respectively. Then both (μ) and (η) are close to being identity matrices. If in addition we

align the sensor and geographic coordinate systems as closely as possible, the matrix (R) is also nearly the identity matrix. Thus the expression $[(\mu)^T\ (R)(\eta)]$ is also close to (I) and we expect the measured field $\underset{\sim}{B}_i$(MEA) to have a large component in the axis nearly aligned with the calibration coil and small components orthogonal to this direction.

We can combine the results of the three successive measurements into a single matrix equation

$$(B_m) = [\mu^T\ R\eta]\ (B_c) \tag{30}$$

where the three vectors $\underset{\sim}{M}_i$ form the columns of (B_M) and $\underset{\sim}{B}_i$(COIL) the columns of (B_c). The matrix (B_c) is diagonal by our choice of calibration procedure

$$(B_c) = \begin{pmatrix} B_1 & 0 & 0 \\ 0 & B_2 & 0 \\ 0 & 0 & B_3 \end{pmatrix}$$

The matrix (B_m) is approximately diagonal

$$(B_m) = \begin{pmatrix} B_{11} & B_{12} & B_{13} \\ B_{21} & B_{22} & B_{23} \\ B_{31} & B_{32} & B_{33} \end{pmatrix}$$

according to eq. (6a)

$$B(SEN) = (\mu^T)^{-1}\ M \tag{31}$$

so solving eq. (30) for $(\mu^T)^{-1}$ we obtain

$$(\mu^T) - 1 = R\ \ (B_m B_c^{-1})^{-1}$$

The matrix $(B)_c$ is diagonal hence its inverse has elements which are the reciprocals of the elements of (B_c). Furthermore, post multiplication of a matrix (B_m) by a diagonal matrix is equivalent to multiplying each column of (B_m) by the corresponding diagonal element. Thus

$$(b) = B_m B_c^{-1} = \begin{pmatrix} B_{11}/B_1 & B_{12}/B_2 & B_{13}/B_3 \\ B_{21}/B_1 & B_{22}/B_2 & B_{23}/B_3 \\ B_{31}/B_1 & B_{32}/B_3 & B_{33}/B_3 \end{pmatrix} \tag{32}$$

The matrix (b) is constructed by normalizing the three sensor measurements in each experiment by the corresponding calibration field. Thus,

$$(\mu^T)^{-1} = R\eta\, b^{-1} \tag{33}$$

Errors in Magnetic Axis Orientation Given Direction Cosines of the Calibration Coils

The preceding result suggests that the direction cosines of the coils are quite easily measured if the direction cosines of the calibration coils are known. The magnetometer array is aligned with the calibration coils, three calibration fields are applied in three successive axes, and the resulting magnetometer measurements are used to calculate the matrix (μ) according to eq. (32). A consideration of errors in this procedure, however, indicates that this simple procedure must be modified somewhat.

To examine the errors in (33) we write each of the measured matrices as the sum of the true matrix and an error matrix.

$$(R) = (R^\circ) + (\varepsilon^R)$$
$$(\eta) = (\eta^\circ) + (\varepsilon^\eta)$$
$$(b^{-1}) = (b^{-1})^\circ + (\varepsilon^b)$$

thus

$$(\mu^T)^{-1} = (R^\circ + \varepsilon^R)\,(\eta^\circ + \varepsilon^\eta)\,((b^{-1})^\circ + \varepsilon^b)$$

or

$$(\mu^T)^{-1} = R^\circ\eta^\circ(b^{-1})^\circ + [R^\circ\varepsilon^\eta(b^{-1})^\circ + \varepsilon^R\eta^\circ(b^{-1})^\circ + R^\circ\eta^\circ\,\varepsilon^b]$$

where we neglect terms of second and third order in the error matrices.

$$(\mu^{T})^{-1} = R \circ \eta \circ (B^{-1}) \circ + [\varepsilon^{R} + \varepsilon^{\eta} + \varepsilon^{b}] \qquad (34)$$

The errors in any element of (μ) is approximately the sum of the errors in the elements of the measured matrices. Consider first the effect of magnetic field measurement errors (ε^{B}). The magnetometer output in a noisey test site will fluctuate by about $\pm$ 1γ. If our calibration field magnitude is 50,000γ, the error matrix (ε^{B}) will have elements of order $\pm$ 1/50,000 = $\pm$ .00002. Let us suppose this error occurs in an element that should be exactly 0.0, i.e. the magnetic axis is exactly orthogonal to one of the geometric axes of the sensor assembly. Then the angular error in the orientation of the magnetometer axis is

$$\delta\theta \approx \frac{1}{2} [\text{Arc Cos } (-.00002) - \text{Arc Cos } (+.00002)]$$

or

$$\delta\theta = .00114^{\circ} = 4''$$

The calibration error in (μ) due to this source alone exceeds the design goal of one arc second. We note that if the site and instrument are both quiet, quantization error will probably be of this order. Note that 1γ resolution in $\pm$ 65 Kγ requires a 17 bit converter on the magnetometer output.

Errors due to the transformation from geographic to sensor coordinates are expected to be small. Large dynamic range autocollinators have accuracies of order one arc second (Schneider and Kolany, 1967).

The largest error is likely to be due to measurement of the direction cosines of the calibration coils. For example, a magnetic theodolite such as that shown in Figure 3 has an accuracy of about 6 arc seconds. More elaborate versions of this instrument described by Yanagihara, 1973, have accuracies of 3" and 1".

If we suppose we use the best magnetic theodolite to determine (η), a wide dynamic range autocollimator to determine (R) and improve our magnetic field measurement to correspond to one arc second, our errors in (μ) are still or order 3". In a 50,000γ field this corresponds to about 0.7γ.

To achieve the equivalent of one arc second accuracy in the magnetic field measurements of this calibration procedure we require $\delta B \simeq 0.2\gamma$. But $0.2/2(50,000) = 2 \times 10^{-6}$ or 1 part in 500,000. This is about one bit in 2^{19}. The best available digital voltmeters have an absolute accuracy of about 50μV in 10 volts or 1 part in 200,000. Thus, neither a digital magnetometer using a 16 bit converter nor an analog magnetometer using the best available digital voltmeter will provide sufficient measurement accuracy to give the equivalent of one arc second accuracy in the determination of (μ).

From the preceding argument it appears necessary to make repeated measurements of the field to obtain the necessary accuracy through averaging. However, because of the quantization problem discussed above, this may not work. Since instrument noise, and possibly test site noise, may both be smaller than the quantization level, the actual magnetometer output may not be uniformly distributed within the quantization interval. In such situations repeated measurements do not increase accuracy.

To eliminate the foregoing problem, and also to improve the signal to site noise ratio, we propose the following. All three calibration coils are simultaneously driven in phase by a sinusoidal current of precisely known frequency ($\simeq$0.1 Hz). A large amplitude signal (50,000γ) is used in one axis as before, and small amplitudes are used

in the remaining two axes (10γ). The drive currents and magnetometer outputs are monitored by a digital data acquisition system for 100 cycles (20 minutes). The amplitude and phase (should be zero) of all signals is determined by least square fitting of a sine wave of the known drive frequency to the measured data.

The small fields used in the two coils orthogonal to the main drive coil will force the magnetometer signals in the corresponding axes to cross several quantization levels. In this manner, the small fields produced in these axes by the main calibration field can be accurately measured because of a uniform distribution of the sensor outputs across a quantization level.

It should be noted that using this procedure the calibration matrix (B_c) constructed from the measured amplitudes is no longer diagonal. As a consequence, we must use matrix methods to determine the matrix,

$$b = (B_m B_c^{-1})$$

With this modification the procedure outlined at the beginning of the section should be adequate.

Determination of Magnetic Axes and Coil Axes Simultaneously

If we assume that the direction cosines of the calibration coils are unknown we can still use eq. (12) to determine the orientation of the magnetic axes as well as those of the coils. In this case eq. (12) constitutes three equations for 18 unknowns. If as before we apply three calibration fields in three orthogonal directions we have (eq) 30 which is a set of 9 equations for 18 unknowns. If we include the unit vector constraint on each column of (μ) and (η) we still have 12 unknowns. Clearly there is insufficient information to solve for the unknowns.

Additional information can be obtained by reorienting the sensor assembly with respect to the calibration coils. This changes the elements of (R) relating the unknowns to the measurements. Using the superscript α to designate the particular orientation of sensor and geographic coordinates, eq. (30) can be written

$$[\mu^T R_\xi] = (B_M^\alpha)\,(B_C^\alpha)^{-1} \qquad \alpha = 1, 2, \ldots \tag{35}$$

For example, using two orientations we should have a set of 18 non-linear equations for 18 unknowns.

It should be noted that successive orientations should be as different as possible. For example if R^1 and R^2 are very close to each other, very little new information would be provided by a second set of measurements. In the presence of errors it would then be impossible to solve the equations for (μ) and (η).

If we expand the ij^{th} element of equation (35) we obtain

$$\sum_{\lambda=1}^{3}\sum_{\mu=1}^{3} R_{\lambda\mu}{}^{\alpha}\,\mu_{\lambda i}\,\eta_{\mu j} = \sum_{\lambda=1}^{3} (B_m{}^{\alpha})_{i\lambda}\,(B_c{}^{\alpha})_{\lambda j}{}^{-1} \tag{36}$$

where α - 1, 2, ...N and i and j = 1, 2, 3.

In a subsequent section we show how this set of equations may be solved by an iterative procedure using a Taylor series expansion which linearizes equation (36).

A procedure for determining the direction cosines of a single calibration coil and one sensor

The solution of the set of equations defined by equation (36) is a complex procedure. Furthermore it requires that the orthogonal sensor array be rotated relative to the calibration coils. In some cases this may not be possible to do. However, if we can determine the direction cosines of the calibration coils in separate experiments we can use the procedure described above to obtain the magnetic axes of the sensor. In this section we will show how a single sensor may be used to determine the direction cosines of one calibration coil. In subsequent sections we generalize this method to the case of three sensors and three coils.

Let $\hat{m}_i$ be the unit vector defining the magnetic axis of the sensor in sensor coordinates, $\hat{n}_j$ the unit vector defining the calibration coil axis in geographic coordinates and B_j the magnitude of the calibration field. The output of the sensor is given by

$$M_{ij} = \hat{m}_i \cdot \underset{\sim}{B}_j$$

where $\underset{\sim}{B}_j$ must be defined in sensor coordinates. But $\underset{\sim}{B}_j = B_j \hat{n}_j'$ with $\hat{n}_j'$ being the representation of $\hat{n}_j$ in sensor coordinates. Thus

$$M_{ij}/B_j = \hat{m}_i \cdot \hat{n}_j'$$

considering $\hat{m}_i$ and $\hat{n}_j'$ as column vectors we can rewrite the dot procuct

$$M_{ij}/B_j = \sum_{\alpha} m_{\alpha i}\, n_{\alpha j}' = \sum_{\alpha} (m^T)_{i\alpha}\, n_{\alpha j}$$

But $\underset{\sim}{V}(SEN) = (R)\ \underset{\sim}{V}(GEO)$

so that

$$\hat{n}_j' = (R)\,\hat{n}_j$$

or

$$n'_{\alpha j} = \sum_{\beta} R_{\alpha\beta}\, n_{\beta j}$$

Hence

$$M_{ij}/B_j = \sum_{\alpha}\sum_{\beta} (m^T)_{i\alpha} R_{\alpha\beta} n_{\beta j}$$

or

$$\sum_{\alpha}\sum_{\beta} R_{\alpha\beta}\, m^T_{i\alpha}\, n_{\beta j} = M_{ij}/B_j \qquad (37)$$

This equation is identical to eq. (36) when the calibration matrix (B_c) is diagonal, i.e. only one calibration coil is excited in any one measurement.

Since i and j are fixed there are six unknowns in eq. (37). To solve for them we must perform at least six different experiments with the sensor $\hat{m}_i$ taking different orientations relative to the calibration coil $\hat{n}_j$. Using (γ) to designate each of these experiments we have

$$\sum_{\alpha}\sum_{\beta} R_{\alpha\beta}(\gamma)\, m_{\alpha i}\, n_{\beta j} = M_{ij}(\gamma)/B_j(\gamma)$$
$$\gamma = 1, 2, \ldots N \qquad (38)$$

To linearize this equation we assume that we know the orientations of $\hat{m}_i$ and $\hat{n}_j$ to about one degree. This is reasonable since both the coil axes and magnetic axes can be manufactured with this accuracy. Thus we take initially,

$$m_{\alpha i} \simeq m^0_{\alpha i}$$
$$n_{\beta j} \simeq n^0_{\beta j} \qquad (39)$$

We then make a Taylor series expansion of the left hand side of (38) about this initial model, obtaining

$$M_{ij}(\gamma)/B_j(\gamma) \cong A_\gamma(\hat{x}^0) + \sum_{\lambda=1}^{6} \left.\frac{\partial A_\gamma}{\partial x_\lambda}\right|_{\hat{x}^0} \delta x_\lambda \qquad (40)$$

In this expansion $\hat{\mathbf{x}}$ is a six component column vector constructed from the two unknown vectors, i.e.

$$\hat{\mathbf{x}} = \begin{pmatrix} \hat{\mathbf{m}} \\ \hat{\mathbf{n}} \end{pmatrix}$$

Thus

$$\hat{\mathbf{x}}^0 = \begin{pmatrix} \hat{\mathbf{m}}^0 \\ \hat{\mathbf{n}}^0 \end{pmatrix} \equiv \text{the initial model}$$

$$\Delta\underset{\sim}{\mathbf{x}} = \begin{pmatrix} \Delta\underset{\sim}{\mathbf{m}} \\ \Delta\underset{\sim}{\mathbf{n}} \end{pmatrix} \equiv \text{corrections to the initial model}$$

Hence, $A_\gamma(\hat{x}^0) = \sum_\alpha \sum_\beta R_{\alpha\beta}(\gamma)\, m^0_{\alpha i}\, n^0_{\beta j}$

The derivatives are given by

$$\left.\frac{\partial A_\gamma}{\partial m_{\lambda i}}\right|_{\hat{x}^0} = \sum_\alpha \sum_\beta R_{\alpha\beta}(\gamma) \left.\frac{\partial m_{\alpha i}}{\partial m_{\lambda i}}\, n_{\beta j}\right|_{\hat{x}^0}$$

but

$$\frac{\partial m_{\alpha i}}{\partial m_{\lambda i}} = \begin{cases} 1 & \alpha = \lambda \\ 0 & \alpha \neq \lambda \end{cases}$$

so that

$$\left.\frac{\partial A_\gamma}{\partial m_{\lambda i}}\right|_{\hat{x}^0} = \sum_\beta R_{\lambda\beta}(\gamma)\, n^0_{\beta j}$$

Similarly we find

$$\left.\frac{\partial A_\gamma}{\partial n_{\lambda j}}\right|_{\hat{x}^0} = \sum_\beta R_{\beta\lambda}(\gamma)\, m^0_{\beta i}$$

Substituting into eq. (40) gives

$$M_{ij}(\gamma)/B_j(\gamma) = \sum_\alpha \sum_\beta R_{\alpha\beta}(\gamma)\, m^0_{\alpha i}\, n^0_{\beta i} + \sum_{\lambda=1}^{3} \left(\sum_\beta R_{\lambda\beta}(\gamma)\, n^0_{\beta j}\right) \Delta m_{\lambda i} + \sum_{\lambda=1}^{3} \left(\sum_\beta R_{\beta\lambda}(\gamma) m^0_{\beta i}\right) \Delta n_{\lambda j} \qquad (41)$$

We may simplify eq. (41) by the use of the matrix notation.

Let

$$b_{ij}(\gamma) = M_{ij}(\gamma)/B_j(\gamma)$$

Then

$$b_{ij}(\gamma) = (\hat{m}^o_i)^T \cdot (R(\gamma)\hat{n}_j^o) + (R(\alpha)\hat{n}_j^o) \cdot \Delta\hat{m}_i + (R^T(\alpha)\hat{m}_i^o) \cdot \Delta\hat{n}_j \qquad (42)$$

This equation may be interpreted physically as follows. The left side is the normalized measurement of the i^{th} sensor in response to the j^{th} calibration coil. The first term on the right hand side is the predicted, normalized response when we use the initial model for the orientations of the sensor and coil. The second term on the right hand side is the projection of the initial coil axis on the correction to the sensor axis in sensor coordinates. The third term is the projection of the initial sensor axis on the correction to the coil axis in geographic coordinates.

If we move the first term of the rightside to the left we obtain

$$(R(\alpha)\hat{n}^o) \cdot \Delta\hat{m}_i + (R^T(\alpha)\hat{m}^o) \cdot \Delta\hat{n}_j = b_{ij}(\gamma) - [(\hat{m}^o)^T \cdot R(\gamma)\hat{n}^o] \quad \text{for } \gamma = 1, 2, \ldots N \qquad (43)$$

In this form, we clearly have a set of N linear equations in the six unknowns, $\Delta\hat{m}$, $\Delta\hat{n}$. The form of this equation is

$$\sum_{\xi=1}^{3} A_{\gamma\xi} X_\xi = Y_\gamma \qquad \gamma = 1, 2, \ldots N \qquad (44)$$

where X_ξ are the elements of the correction vectors $\Delta\hat{m}$, $\Delta\hat{n}$; Y_γ is the difference between the measured and predicted values of the normalized measurements; and $A_{\gamma\xi}$ is an (N x 6) matrix with rows constructed from the initial coil axis in sensor coordinates and the initial sensor axis in geographic coordinates.

We solve the set of N eq's (43) in an iterative manner. An initial guess is made for the direction cosines of $\hat{m}_i$ and $\hat{n}_j$. By construction these are designed to be as nearly aligned with the corresponding axes of sensor and geographic coordinates. Thus the initial guess is

$$(\hat{m}_i^o)_\alpha = \delta_{i\alpha} \quad \text{and} \quad (\hat{n}_j^o)_\alpha = \delta_{j\alpha}$$

Evaluating the constant terms in eq. (43) we obtain a set of equations of the form (44). These equations are solved for the correction vectors $\Delta\hat{m}^1_i$,

$\Delta\hat{n}^1_j$ by the method discussed below. The corrections are added to the initial guess to obtain a new starting model. Thus

$$\hat{m}_i^{\,1} = \hat{m}^o_i + \Delta\hat{m}^1$$

$$\hat{n}_j^{\,1} = \hat{n}_j^{\,o} + \Delta\hat{n}^1_j$$

Using these new vectors as a starting model, we repeat the procedure obtaining a second set of solutions $\hat{m}_i^{\,2}$, $\hat{n}_j^{\,2}$. Provided the initial model is close to the correct model, the problem is nearly linear and the sequence of corrections converge rapidly to zero.

Solution of the set of N equations and M unknowns

In the preceding section we showed the problem of simultaneously determining the direction cosines of sensor and coil could be reduced to a problem of solving N linear equations for six unknowns. Thus we solve

$$\sum_{\xi=1}^{m} A_{\gamma\xi} X_{\xi} = Y_{\gamma} \qquad \gamma = 1, 2, \ldots N \tag{44}$$

for the m (m = 6) unknowns X_{ξ}. In matrix form this may be written

$$(A)\underset{\sim}{x} = \underset{\sim}{y}$$

A general procedure for doing this has been described by Lanazos, 1961 (p. 100-162). We briefly summarize this procedure below.

Let (A) be the (N x M) matrix of coefficients in equation (44). Construct the (N x N) symmetric matrix AA^T and the (M x M) symmetric matrix A^TA. Solve the two eigenvalue problems

$$\begin{aligned} AA^T u &= \lambda^2 u \qquad \text{N eigenvalues} \\ A^TA v &= \lambda^2 v \qquad \text{M eigenvalues} \end{aligned} \tag{45}$$

Construct two matrices U and V from the eigenvectors u and v. The matrix U is (N x N) and V is (M x M). At most there will be only p, non-zero eigenvalues λ_i where $p \leq \min(N,M)$. The non-zero eigenvalues are the same for both AA^T and A^TA

Now construct an (N x P) matrix U_p and an (N x (N-P)) matrix U_o by partitioning U into two matrices having columns corresponding to non-zero and zero eigenvalues respectively. Similarly construct an (M x P) matrix V_p and an (N x (M-P)) matrix V_o from V. The matrices U_p, V_p diagonalize the matrix A by the transformation

$$\Lambda_p = U_p^T A V_p \tag{46}$$

where Λ_p is a p x p matrix with diagonal elements corresponding to the square

roots of the non-zero eigenvalues of eq. (45). From (46) we have

$$A = U_p \Lambda_p V_p^T \qquad (N \times M) \qquad (47)$$

The natural inverse of (A) is given by

$$B = V_p \Lambda_p^{-1} U_p^T \qquad (M \times N) \qquad (48)$$

$$\begin{aligned} AB &= UU^T \\ BA &= VV^T \end{aligned} \qquad (49)$$

The solution to our set of equations (44) is then as follows

$$\begin{aligned} Ax &= y \\ (U_p \Lambda_p V_p^T)\, x &= y \\ x &= (V_p \Lambda_p^{-1} U_p^T) y \\ x &= (B) y \end{aligned} \qquad (50)$$

The solution, eq. (50), always exits, but it will not necessarily be a good one. First, some eigenvalues λ_i may be non-zero but small. In this case, corresponding elements in the inverse matrix Λ_p^{-1} will be very large. As a consequence, very small errors in the constant vector y will be magnified in the solution vector x.

A second problem is that errors made in the measurement of A and the vector y may make the equations incompatible. Lanczos shows the set of equations are compatible only if

$$U_o^T y = 0 \qquad (51)$$

Physically this implies that the constant vector y must be orthogonal to all eigenvectors corresponding to zero eigenvalues.

Finally, the set of equations may be deficient. In this case they contain insufficient information to determine certain linear combinations of the unknowns. These combinations are given by

$$V_o^T \eta \qquad (52)$$

where V_o is the matrix of zero eigenvectors from the matrix V and $\underline{r}$ is an arbitrary column vector.

Computer simulation of the simultaneous determination of the orientations of a single sensor and single coil - no constraints

To test the procedure described in the preceding two sections, we have used a computer program to simulate an actual calibration experiment. Inputs to this simulation program are the direction cosines of the coil and sensor in their respective Cartesian coordinate systems and six transformation matrices corresponding to different orientations of the sensor relative to the coil. Outputs from the simulation program are the normalized magnetometer measurements which would have been made in the absence of measurement errors.

Six different sensor orientations were used as summarized in Figure 8. For this experiment, the sensor was chosen to be along the x axis of sensor coordinates and the coil along the z axis of geographic coordinates. The nine different transformation matrices and the corresponding normalized sensor measurements are presented in Table 1. A listing of the simulation program is included as Appendix A2.

The second step in the simulation required a computer program which implements the procedure described in the preceding two sections. This program was written in the IBM-TSO (Time Sharing Option) version of SPEAKEZ. This language was written and is maintained by the Argonne National Laboratory (Cohen and Pieper, 1976). It is especially designed to facilitate the manipulation of vectors and matrices. A listing of the latest version of this program (MAGCAL1) is included as Appendix A3.

The results obtained by this program were quite satisfactory, converging to nearly correct values after at most three iterations. A representative result using five measurements

$$\hat{M}_x^1 = (.99935, .030011, .039929)$$

as compared to the known input,

$$\hat{M}_x = (.99375, .030000, .040000)$$

While the foregoing procedure is successful it is difficult to carry out experimentally. The problem is that it is exceedingly difficult to perform the measurements necessary to calculate the transformation matrix (R). Thus the most desirable procedure is one which minimizes the number of different orientations of sensor and coil.

One method of reducing the number of necessary orientations is to take advantage of the unit vector constraints. Since both $\hat{m}_i$ and $\hat{n}_j$ are unit vectors there are only four unknowns rather than six. Hence only four orientations should be required.

Utilization of the unit vector constraint to reduce the number of experimental measurements

Thus far we have not used the constraint that both $\hat{m}_i$ and $\hat{n}_j$ should be unit vectors. This constraint can be included in two ways. The most straight forward way is to linearize the constraint equations and include them in the set of linearized equations solved by the computer procedure. A second way is to use the constraints directly to eliminate two unknowns from eq. (38) and then linearize these modified equations. We find empirically that only the second method works. Basically, the reason appears to be a result of losing too much information in separately linearizing the fundamental equation (38) and the constraints.

To include the unit vector constraint directly we return to the original equation describing the result of any particular measurement, eq. (38).

$$\sum_{\alpha}\sum_{\beta} R_{\alpha\beta}(\gamma)\, m_{\alpha i}\, n_{\beta j} = M_{ij}(\gamma)/B_j(\gamma) \qquad \gamma = 1, 2, \ldots N \tag{38}$$

Since $\hat{m}$ and $\hat{n}$ are unit vectors we have

$$\sum_{\alpha}(m_{\alpha i})^2 = 1 \quad \text{and} \quad \sum_{\alpha}(n_{\alpha j})^2 = 1$$

we may solve these for the diagonal elements

$$m_{ii} = \sqrt{1 - \sum_{\alpha \neq i} (m_{\alpha i})^2}$$
$$n_{jj} = \sqrt{1 - \sum_{\alpha \neq j} (n_{\alpha j})^2} \qquad (53)$$

while these can be substituted directly in eq. (38) it is not necessary to do so. Instead, we treat eq. (38) as before as a function of six variables, i.e.

$$f(m_{xi}, m_{yi}, m_{zi}, n_{xj}, n_{yj}, n_{zj})$$

but utilize the rules for implicit differentiation to evaluate the derivatives of the diagonal elements. Thus,

$$f \cong f_{(\hat{x}_0)} + df\Big|_{\hat{x}_0} \qquad (54)$$

where

$$df = \sum_{\alpha=1}^{3} \frac{\partial f}{\partial m_{\alpha i}} dm_{\alpha i} + \sum_{\alpha=1}^{3} \frac{\partial f}{\partial n_{\alpha j}} dn_{\alpha j} \qquad (55)$$

Isolating the diagonal element in each sum gives

$$df = \sum_{\alpha \neq i} \frac{\partial f}{\partial m_{\alpha i}} dm_{\alpha i} + \frac{\partial f}{\partial m_{ii}} dm_{ii} + \sum_{\alpha = j} \frac{\partial f}{\partial n_{\alpha j}} dn_{\alpha j} + \frac{\partial f}{\partial n_{jj}} dn_{jj} \qquad (56)$$

From equations (54 & 55) the total derivatives of the diagonal elements are

$$dm_{ii} = \sum_{\alpha \neq i} \frac{\partial m_{ii}}{\partial m_{\alpha i}} dm_{\alpha i}$$
$$dn_{jj} = \sum_{\alpha \neq j} \frac{\partial n_{jj}}{\partial n_{\alpha j}} dn_{\alpha j}$$

Substituting in eq. (56) gives

$$df = \sum_{\alpha = i} \left(\frac{\partial f}{\partial m_{\alpha i}} + \frac{\partial f}{\partial m_{ii}} \frac{\partial m_{ii}}{\partial m_{\alpha i}}\right) dm_{\alpha i}$$
$$+ \sum_{\alpha \neq j} \left(\frac{\partial f}{\partial n_{\alpha j}} + \frac{\partial f}{\partial n_{jj}} \frac{\partial n_{jj}}{\partial n_{\alpha j}}\right) dn_{\alpha j} \qquad (57)$$

Since α takes on only two values in each sensor we have clearly reduced the number of unknowns from six to four. The remaining two unknowns are defined

by the equation (53). Since

$$f = \sum_{\lambda} \sum_{\mu} R_{\lambda\mu}(\gamma)\, m_{\lambda i}\, n_{\mu j} \tag{58}$$

we may evaluate the derivatives in (57). Thus

$$\frac{\partial f}{\partial m_{\alpha i}} = \sum_{\mu} R_{\alpha\mu}(\gamma)\, n_{\mu j} = (R\,\hat{n}_j)_\alpha$$

$$\frac{\partial f}{\partial n_{\alpha j}} = \sum_{\lambda} R_{\lambda\alpha}(\gamma)\, m_{\lambda i} = (R^T \hat{m}_i)_\alpha$$

$$\frac{\partial m_{ii}}{\partial m_{\alpha i}} = -\frac{m_{\alpha i}}{m_{ii}} \qquad \alpha \neq i$$

$$\frac{\partial n_{jj}}{\partial n_{\alpha j}} = -\frac{n_{\alpha j}}{n_{jj}} \qquad \alpha \neq j$$

Hence the quantities within parenthesis in equation (57) are

$$\left[\frac{\partial f}{\partial m_{\alpha i}} + \frac{\partial f}{\partial m_{ii}} \cdot \frac{\partial m_{ii}}{\partial m_{\alpha i}}\right] = \left[(R\hat{n}_j)_\alpha - (R\hat{n}_j)_i \left(\frac{m_{\alpha i}}{m_{ii}}\right)\right]$$

$$\left[\frac{\partial f}{\partial n_{\alpha j}} + \frac{\partial f}{\partial n_{jj}} \cdot \frac{\partial n_{jj}}{\partial n_{\alpha j}}\right] = \left[(R^T\hat{m}_i)_\alpha - (R^T\hat{m}_i)_i \left(\frac{n_{\alpha j}}{n_{jj}}\right)\right]$$

These derivatives must be evaluated for the initial model, i.e. $\hat{m}_i$ and $\hat{n}_j$ are replaced by the guesses $\hat{m}_i^o$ and $\hat{n}_j^o$ in the above expressions. Then, proceeding as we did in the derivation of eq. (43) we find

$$\sum_{\alpha \neq i} \left[(R\hat{n}_j^o)_\alpha - (R\hat{n}_j)_i \left(\frac{m^o_{\alpha i}}{m^o_{ii}}\right)\right] \Delta m_{\alpha i}$$

$$+ \sum_{\alpha \neq j} \left[(R^T\hat{m}_i^o)_\alpha - (R^T\hat{m}_i^o)_i \left(\frac{n^o_{\alpha j}}{n^o_{jj}}\right)\right] \Delta n_{\alpha j}$$

$$= M_{ij}/B_j - [(\hat{m}^o)^T \cdot R\hat{n}^o] \tag{59}$$

Note for convenience we have not indicated the dependence of R, M_{ij} and B_j on (γ), the relative orientation of sensor i and coil j.

This expression is very similar to eq. (43) except it no longer has an obvious physical interpretation because we have explicitly included

the unit vector constraint. The major difference is the reduction of the number of unknowns from six to four. Thus the equation now has the form

$$(A)\quad x = y \qquad = 1, 2, \ldots N \tag{60}$$

These equations may be solved by exactly the same method as used before. The only changes required are in the dimensionality of the (A) matrix and the calculation of its elements.

Computer simulation including constraints

The procedure described in the previous section was implemented by making slight modifications in the program MAGCAL. A listing of the new program MAGCAL1 is included as Appendix A3. This program was tested using the same data as were used to test MAGCAL (c.f. Table 1). On a basis of this test we conclude the second procedure is far superior to the first.

We find that the inclusion of the unit vector constraint improves the rate of convergence, improves the accuracy and reduces the number of necessary measurements. A sample result obtained after two iterations was

$$\hat{m}_x = (.99875, .030000, .039996)$$

$$\hat{n}_z = (.010001, .020006, .99975)$$

These should be compared to the known values

$$\hat{m}_x = (.99875, .030000, .040000)$$

$$\hat{n}_z = (.010000, .020000, .999750)$$

Similarly good results were obtained using only four experiments, provided experiment number 3 of Table 1 was not included. This experiment corresponds to alignment of the sensor with the calibration coil.

This unexpected result suggests that some sensor orientations are better than others for determining the direction cosines of sensor and coil.

We interpret this result in the following fashion. The function

$$f = \sum_{\alpha}\sum_{\beta} R_{\alpha\beta}\, m_{\alpha i}\, n_{\beta j} = b_{ij}$$

is a maximum for a matrix R corresponding to alignment of $\hat{m}_i$ and $\hat{n}_j$. Our method of linearizing the equation to solve for $\hat{m}_i$, $\hat{n}_j$ utilizes the derivatives of f as a function of the elements of $\hat{m}$ and $\hat{n}$ to calculate corrections in the initial guess. Since our initial guess corresponds to exact alignment the initial derivatives should be exactly zero. Thus there is no way to calculate a correction to the initial guess.

Examination of the eigenvalues obtained in the solution of the set of four equations for this computer simulation shows that one of the four eigenvalues was much smaller than the remaining three. This implies that there are fewer equations than unknowns and therefore the equations are not really soluble. Clearly the data obtained in experiment 3 by near alignment of sensor and coil does not contribute much information.

Errors in magnetic axes orientation using simultaneous determination procedure

In our procedure for simulatneous determination of sensor and coil axis we utilized the Lanczos inverse. Thus

$$Ax = y$$

has a solution

$$\hat{x} = By$$

where $B = V_p, \Lambda_p^{-1} U_p^T$

As discussed by Jackson, 1972, the errors in the solution vector $\hat{x}$ are given by

$$\text{Var}\,(\hat{x}_k) = \sum_{i=1}^{n} (B_{ki})^2 \,\text{Var}\,(y_i) \qquad (61)$$

Since B_{ki} depends on the reciprocal eigenvalues of Λ_p^{-1} any small eigenvalues will cause very large errors in all components of the solution vector. Equation (61) may be written in matrix form as

$$\text{Var}\,(\hat{x}) = (B^2)\,\text{Var}\,(\hat{y}) \qquad (62)$$

In this relation B^2 is a matrix whose elements are the squares of the elements of B. Var $(\hat{x})$ and Var $(\hat{y})$ are vectors constructed from the respective component variances.

To obtain some idea of the errors to be expected in our simultaneous determination procedure we have included eq. (62) as part of program MAGCAL and MAGCAL1 For the simulation described in the preceding section (four experiments using constraints) we find the following results.

First we assume the variance of all input measurements to be the same, and roughly of order 1 gamma in 50,000 γ, i.e. $VAR(y_i) \approx (1/50,000)^2$. Then from eq. (61)

$$\text{Var } (\hat{x}_k) = VAR(y) \cdot \sum_i (B_{ki})^2$$

A typical row in the matrix (B^2) was for our first simulation

(.5, 3.0, 1.0, 5.5)

which sums to 10. Thus the expected variance in the solutions is roughly ten times that of the input data. Hence

$$VAR\ (x_k) \approx 10\ (1/50,000)^2$$

Or RMS error in $x_k \sim 6 \times 10^{-5}$.

To convert this to angular measure we note

$$\cos \theta = n_{zy} = .02 \pm 6 \times 10^{-5}$$

and

$$\delta\theta \simeq \text{Arc cos}(.02 \pm 6 \times 10^{-5}) - \text{Arc cos } (.02)$$

or

$$\delta\theta \simeq 3.4 \times 10^{-3} = 12 \text{ arc seconds.}$$

This error is quite large compared to the design goal of one arc second.

One possible means of reducing this error is to reduce the magnitude of the elements of the inverse matrix. Since this depends on the original matrix (A) which in turn depends on the relative orientation of sensor and coil, it is possible that a different set of four experiments would provide a more accurate determination.

To check this possibility we have performed a second simulation using the four orientations shown in figure 9 and Table 2. To decide on which orientations to use we guessed that large elements of the inverse B depend on small elements of A. Apart from zero elements, the smallest elements of A arise from the 45° relative orientations. We thus decided to use only 90° rotations to obtain the four orientations shown in figure 9.

The results from this second simulation were quite surprising. We found

$$MAX\ (RMS\ (x_k)) \simeq 2.5 \times 10^{-5}$$

This is more than a factor of two improvement over the first set of four orientations. The corresponding angular accuracy is of order 6 arc seconds.

While an error of six arc seconds does not meet the design goal it is at least as good as can be expected if the coil cosines are determined with a conventional magnetic theodolite. This error might be further reduced by using the results of an initial determination to design an optimum set of four measurements. It could be reduced still further by repeating the set of four measurements a number of times.

Calibration of Three Sensors Using Three Calibration Coils

In the preceding section we showed how a single sensor could be calibrated using only one coil. This procedure requires a sufficient number of relative orientations of the sensor and coil to define all of the unknowns. In this section we show how the use of three coils makes it possible to calibrate three sensors with the same number of orientations.

Let us assume as before, that for each sensor orientation we carry out three measurements. Each measurement is the vector output of the sensor assembly for a given calibration field. The expected fields for this set of three measurements may be written

$$(B_m) = [\mu^T R \eta] (B_c) \tag{30}$$

where B_m and B_c are 3 x 3 matrices with column corresponding to the three measured and calibration fields respectively This may be written

$$\mu^T R\eta = b \tag{63}$$

where $b = (B_m)(B_c)^{-1}$ is the "normalized" observation matrix.

To linearize this set of equations for μ and η we assume an approximate model is know, i.e. $\mu \approx \mu_o$ and $\eta \approx \eta_o$. We then write μ and η as small perturbations about this known model, thus

$$\mu = \mu_o + \delta\mu$$

$$\eta = \eta_o + \delta\eta$$

Substituting in equation (63) we find

$$(\mu_o{}^T R)\delta\eta + \delta\mu^T (R\eta_o) \cong [b - \mu_o{}^T R\eta_o] \tag{64}$$

where we drop the second order term $\delta\mu^T\delta\eta$ which we assume to be very small.

The righthand side of equation (64) is the difference between the actual measurements (b) and the measurements that would be expected as a result of the initial model. The unknowns $\delta\eta$, $\delta\mu$ on the left hand side are the corrections to the initial model required to obtain better agreement between the observations and the model.

This set of nine equations in eighteen unknowns has the form

$$(A)\ \underset{\sim}{x} = \underset{\sim}{y} \tag{65}$$

Here $\underset{\sim}{x}$ is a column vector with 18 rows constructed from the unknown elements of $\delta\mu$ and $\delta\eta$. The vector $\underset{\sim}{y}$ is a column vector with 9 rows constructed from the residuals between the measured and predicted magnetic field measurements. The matrix (A) is a 9 x 18 rectangular matrix with elements constructed from the two matrices $(\mu_0{}^T R)$ and $(R\eta_0)$. Since this matrix equation constitutes only 9 relations between the 18 unknowns we must obtain additional, linearly independent relationships. We do this by using a different orientation of sensors and coil. Provided these orientations are properly chosen the coefficient matrix will be non-singular and the set of equations will be soluble.

To demonstrate the feasibility of the above approach we have carried out a computer simulation as was done for the single sensor, single coil calibration procedure. Direction cosines of the magnitude expected for sensor and coil were chosen arbitrarily (Table 2). Then equation (63) was used to calculate the expected magnetic field measurements. Seven different orientations of sensors and coils were used as this was the minimum necessary to define all sensor axes when only one calibration coil is used. The seven transformation matrices and the seven calculated measurement matrices were then used as data in the perturbation procedure described above.

To set up the set of nine algebraic equations corresponding to the matrix equation (64) we take the ij^{th} element.

$$\sum_{\alpha=1}^{3} (\mu_o{}^T R)_{i\alpha}\, \delta n_{\alpha j} + \sum_{\alpha=1}^{3} (\delta_\mu{}^T)_{i\alpha}\, (Rn_c)_{\alpha j} = b_{ij} \qquad (66)$$

Clearly, the ij^{th} equation couples only the j^{th} coil axis with the i^{th} sensor, i.e. each equation links only six of the 18 unknowns. Thus if we adopt the convention of first fixing j and then allowing i to run through its range we generate the set of 9 equations shown schematically in Table 5. In Table 5 each column contains the coefficients of the three unknowns associated with a given unit vector. Each row corresponds to successive values of j and i. The entries within this table, i.e. ROW 1, COL 3 refer to rows or columns of the model matrices, $(\mu_o{}^T R)$ and (Rn_o) shown at the bottom left and right sides of the Table. All blank entries correspond to coefficients of zero.

This representation of the set of nine equations is particularly convenient for the computer language, SPEAKEZ. Because this language allows the manipulation of vectors and matrices as entities it is possibly to efficiently define the 9 x 18 coefficient matrix (A) simply by placing the appropriate rows and columns of the model matrices at appropriate locations of (A).

A program which generates the (7*9 x 18) "A" matrix corresponding to the seven orientations of sensor and coil shown in Table 3 was written. The solubility of this set of 63 equations was then tested in the following manner. Assume an initial model corresponding to exact alignment of both sensors and coils in their respective coordinate systems, i.e. μ_o and n_o are identity matrices. Furthermore assume the transformation matrices correspond to exact alignments of the sensor and geographic coordinate systems (not normally the case for actual measurements). With these assumptions the columns of (Rn_o) are the unit vectors of the coils expressed in sensor coordinates. However, because we assume the coils are exactly aligned with

geographic coordinates the columns of $(R\eta_0)$ are actually the unit vectors of geographic coordinates as seen in sensor coordinates. Similarly, rows of $(\mu_0{}^T R)$ correspond to columns of $(R^T\mu_0)$, but by the same arguments as above these are the unit vectors of sensor coordinates as seen in geographic coordinates. Using these facts we can immediately write down the elements of the A matrix by inspection. To decide whether this set of equations can be solved we take the determinant. If this is non-zero the matrix is non-singular and the equations soluble.

For the A matrix based on the seven orientations of Table 3 SPEAKEZ methods showed the determinant was zero. Thus the equations were insoluble. Our interpretation of this result is as follows. The seven orientations of table 3 were deliberately chosen to produce a specific set of four orientations of each sensor relative to one coil. These sets of four orientations were chosen so that the four unknowns associated with one coil and one sensor could be determined. Only four unknowns were present because the unit vector constraints were used to eliminate two of the six unknowns.

This argument leads us to the conclusion that at least several additional orientations would be required to solve for the 18 unknowns by the above method. Because of the experimental difficulties associated with the measurement of the R matrix we rule this out as a viable procedure. Consequently, we extend the foregoing procedure to make use of the six unit vector constraints.

The constraint equations may be written

$$|n_j|^2 = \sum_{\alpha=1}^{3} n_{\alpha j}{}^2 = 1$$
$$|m|_i{}^2 = \sum_{\alpha=1}^{3} m_{\alpha i}{}^2 = 1 \qquad (67)$$

Solving for the diagonal elements we have for columns of (n)

$$n_{jj} = \sqrt{1 - \sum_{\alpha \neq j} n_{\alpha y}^{2}} \tag{68}$$

In our perturbation approximation

$$n_{\alpha j} = n_{\alpha j}^{o} + \delta n_{\alpha j}$$

So that the diagonal elements become

$$n_{jj}^{o} + \delta n_{jj} \equiv [1 - \sum_{\alpha \neq j} (n_{\alpha j}^{o} + \delta n_{\alpha j})^2]^{1/2}$$

Expanding the square and dropping second order terms gives

$$n_{jj}^{o} + \delta n_{jj} \quad [\{1 - \sum_{\alpha \neq j} (n_{\alpha j}^{o})^2\} - 2 \sum_{\alpha \neq j} n_{\alpha j}^{o} \delta n_{\alpha j}]^{1/2}$$

But

$$n_{jj}^{o} = \{1 - \sum_{\alpha} (n_{\alpha j}^{o})^2\}^{1/2}$$

so that

$$n_{jj}^{o} + \delta n_{jj} \simeq n_{jj}^{o} [1 - 2 \frac{\sum_{\alpha \neq j} n_{\alpha j}^{o} \delta n_{\alpha j}}{(n_{jj}^{o})^2}]^{1/2}$$

Because the second term within the brackets is much smaller than one we have

$$n_{jj}^{o} + \delta n_{jj} \simeq n_{jj}^{o} [1 - \frac{\sum_{\alpha \neq j} n_{\alpha j}^{o} \delta n_{\alpha j}}{(n_{jj}^{o})^2}]$$

or finally

$$\delta n_{jj} \simeq - \sum_{\alpha \neq j} (\frac{n_{\alpha j}^{o}}{n_{jj}^{o}}) \delta n_{\alpha j} \tag{69}$$

In an analogous fashion

$$\delta m_{ii} \simeq - \sum_{\alpha \neq j} (\frac{m_{\alpha i}^{o}}{m_{ii}^{o}}) \delta m_{\alpha i} \tag{70}$$

To include these constraints in a modified A matrix we note the following. The two constraints may be written in the form

$$\begin{aligned} -\sum_{\alpha=1}^{3} \left(\frac{n_{\alpha j}^{o}}{n_{jj}^{o}}\right)\delta n_{\alpha j} &= 0 \\ -\sum_{\alpha=1}^{3} \left(\frac{m_{\alpha i}^{o}}{m_{ii}^{o}}\right)\delta m_{\alpha i} &= 0 \end{aligned} \tag{71}$$

Now multiply the first equation by the column of the A matrix corresponding to the unknown δn_{jj}. Similarly multiply the second equation by the column of A corresponding to δm_{ii}. Then, add the two equations obtaining

$$0 = -\sum_{\alpha=1}^{3} \left[\frac{A(\delta n_{jj})}{n_{jj}^{o}} n_{\alpha j}^{o}\right] \cdot \delta n_{\alpha j} - \sum_{\alpha=1}^{3} \left[\frac{A(\delta m_{ii})}{m_{ii}^{o}} m_{\alpha i}^{o}\right] \cdot \delta m_{\alpha i} \tag{72}$$

Finally, add this equation the ij^{th} equation previously obtained without using constraints. (eq. (66)).

When this procedure is carried out explicitly it can be seen that it is exactly equivalent to substituting the constraint equations for the diagonal elements and then rearranging terms. Thus to modify the A matrix shown in Table 5 we must construct a (9 x 18) N matrix with the elements shown in Table 6. Then this matrix (N) must be subtracted from the matrix (A). Subtraction will introduce zeros in the columns of the modified A matrix corresponding to the diagonal elements of the unknown matrices $(\delta\mu)$, $(\delta\eta)$. If we now eliminate all comumns of the modified A matrix corresponding to these diagonal elements we will obtain a new set of equations of the form

$$(AA)\ \underset{\sim}{x}' = \underset{\sim}{y}$$

where now $\underset{\sim}{x}'$ is a column vector with 12 unknowns taken from the off diagonal elements of $(\delta\eta)$, $(\delta\mu)$. $\underset{\sim}{y}$ is a 9 row column vector of residuals between observations and predictions as previously defined. The matrix (AA) is a

(9 x 12) rectangular matrix obtained as described above.

A SPEAKEZ program "EQUATS" was written to implement this procedure. A listing of this program is included as Appendix A5. In the initial text of this program all seven orientations of table 3 were used to construct a (63 x 12) matrix (AA). The determinant of this matrix was found to be non-zero for the particular simulation used. Consequently two additional programs were written to solve for the direction cosines in an iterative fashion.

Program "SOLEQU" (listing also included in Appendix A5), utilizes a SPEAKEZ linkule (similar to subroutine) to solve the set of equations defined by the matrix (AA) and the vector $\underset{\sim}{y}$. This linkule utilizes the singular value decomposition procedure of Lanzcos described earlier. Because this linkule is written to minimize time and storage requirements it does not provide as much information as our own implementation of this procedure embodied in program MAGCAL and MAGCAL 1 (See Appendix A3). However, because our implementation utilizes too much storage we were unable to use it to solve the set of 63 equations.

A second program "MAINPO" was written to implement the iterative perturbation procedure our method of simultaneous solution is based on. This program initiatizes the calculation first reading in the measurements and transformation matrices, and then reading a first guess of the unknowns, (η^0) and (μ^0). Normally we assume these are identity matrices since these are the design goals for both sensors and coils. The program then calls program EQUATS. As its first step program EQUATS increments (μ^0) and (η^0) using previously calculated corrections $(\delta\mu)$ and $(\delta\eta)$. (Initially these are zero). EQUATS then uses the constraint conditions to calculate the diagonal elements of the modified matrices $(\mu^0 + \delta\mu)$ and $(\eta^0 + \delta\eta)$. It then proceeds to generate the matrix (AA) and the vector $\underset{\sim}{y}$. Control is passed to program MAINPO which

calls SOLEQU to solve the set of equations for the vector $\underset{\sim}{x}$. In its final step SOLEQU creates the correction matrices ($\delta\mu$) and (δn) from elements of the solution vector $\underset{\sim}{x}$. Control is returned to program MAINPO which loops back to call program EQUATS. This procedure is repeated the number of times specific during the initiatization phase of program MAINPO.

Results obtained with program MAINPO are comparable to those obtained with the programs which were written to solve the case of one sensor and one coil. For example, the second corrected model was equal to the model used in the simulation program to better than the fifth decimal place.

To determine the minimum number of orientations required to carry out a procedure we progressively reduced the number of different orientations input to program MAINPO. When this number was less than four, the determinant became zero and we were unable to obtain a correct solution to the problem. Although we have only examined the case corresponding to the first four orientations of table 3, we believe that any four orientations satisfying the following criteria would be sufficient to define the 18 direction cosines of (μ) and (n) using our procedure. These criteria are the same as was found for calibrating a single sensor with a single coil: (1) there must be 4 different orientations of the sensor and the coil, (2) direct alignment of the sensor and coil provides no useful information, (3) rotations of 90° from the initial position generate satisfactory orientation provided one rotation brings the sensor axis initially transverst to both coil and sensor parallel to calibration coil.

In summary, our procedure for calibrating the direction cosines of a three axis sensor assembly using a three axis Helmholtz coil system is the following. Attach an optical cube to the sensor assembly. Place the sensor assembly in a fixture that allows 90° rotations about two orthogonal axes and which does not allow the center of the cube to translate during rotation. Begin with an alignment which places the x', y', z' axes of the sensor, i.e. of the optical cube, in near coincidence with the x, y, z axes of the coil, i.e. of geographic coordinates (c.f. Figure 9). Level the fixture using

two theodolites in the horizontal plane on the positive x and y axes of geographyc coordinates. The leveling procedure should be sufficiently accurate to guarantee that theodolite cross hairs remain reflected within their fields of view after successive 90° rotations about the two axes of the fixture. Use the theodolite setting circles to measure the actual orientations of the x' and y' axes of the optical cube to one arc second or better. Apply an accurately known field in the x calibration coil and measure the output of the three sensors. Repeat for the y calibration coil and the z coil using exactly the same field magnitude. From the measurements construct two matrices (B_m) and (B_c) using the successive measurements and calibration fields as columns. Thus.

$$(B_m) = \begin{pmatrix} B_{x1} & B_{x2} & B_{x3} \\ B_{y1} & B_{y2} & B_{y3} \\ B_{z1} & B_{z2} & B_{z3} \end{pmatrix}$$

$$(B_c) = \begin{pmatrix} B_o & 0 & 0 \\ 0 & B_o & 0 \\ 0 & 0 & B_o \end{pmatrix} = B_o(I)$$

Next, calculate the normalized measurement matrix

$$b = (B_m)(B_c)^{-1}$$

which by the choice of calibration fields becomes

$$b = \frac{1}{B_o}(B_m)$$

Now create a nine element column vector of normalized measurements by placing the three columns of the matrix (b) successively beneath each other. Thus

$$\underline{M} = \begin{pmatrix} B_{x1} \\ B_{y1} \\ \vdots \\ B_{y3} \\ B_{z3} \end{pmatrix}$$

Finally, using the orientation angles determined by the theodolites construct the transformation matrix (R) from geographic to sensor coordinates. The (3 x 3) rotation matric (R) and the nine element column vector $\underset{\sim}{M}$ are the data to be input to the simultaneous equation solving program MAINPO.

Having completed the measurements for the first orientation we rotate the sensor assembly + 90° about its z axis (azimuth axis of fixture). The actual orientations of two sensor axes of the sensor assembly are determined by the x and y theodolites as before. We then repeat the previous sequence of three calibration fields and corresponding measurements. A matrix (R) and a vector $\underset{\sim}{M}$ calculated as above form the second set of input data for program MAINPO.

For the third orientation of figure 9 we rotate an additional + 90° about the azimuth axis of the fixture and obtain measurements as before. Finally, the fourth orientation is obtained by a 90° rotation about the elevation axis of the fixture. This brings the top of the optical cube down to a position where it may be viewed by the y theodolite.

After all data have been properly entered into program MAINPO, the program requests an initial guess for the matrices (μ) and (η) defining the direction cosines of the sensors in sensor coordinates and of the coils in geographic coordinates. If no prior information is available these are assumed to be identity matrices. The program then proceeds through several iterations obtaining a final, least square determination of the best fit of the direction cosines of sensors and coils to the input data.

Recommendations

The high absolute accuracy desired for the MAGSAT magnetometer requires accurate calibration equipment and some new procedures. We recommend acquisition

To make an accurate determination of sensor direction cosines, the calibration coil direction cosines must also be determined accurately. This can be done in two ways.

1) With a magnetic theodolite which would need to be purchased

2) Simultaneously as the sensor cosines are determined

In our report we choose the simultaneous determination procedure. We show that this technique should be able to provide accuracy of order 5-10 arc seconds. This accuracy is comparable to that of easily acquired magnetic theodolites. To significantly improve this accuracy would require repeated measurement of the direction cosines. This procedure requires four reorientations of the sensor assembly. For each orientation both theodolites must be read and a series of three calibration fields applied and the magnetometer output recorded.

We recommend that this procedure be automated and placed under the control of a minicomputer. This would require that the rotation fixture have motor control of each axis. Additionally, the theodolites should have digital readouts.

If we accept 10 arc seconds as the obtainable accuracy of the direction cosines of the sensors, then the absolute accuracy of the magnetometer cannot be better than $\pm$ 2 gamma. However, individual sensor errors will also be about $\pm$ 1 gamma, so we expect the final accuracy to be about $\pm$ 3 gamma. Significantly improving this accuracy appears to involve very labor intensive calibration procedures.

of the following equipment:

1) Two optical theodolites of one arc second accuracy
2) Six digit digital voltmeter
3) Two precision levels of one arc second accruacy
4) Smooth, non-magnetic test table of granite or glass
5) Brass fixture for rotating sensor assembly about horizontal and vertical axes with precision of order one minute
6) Minicomputer controller and data logger with video display keyboard entry

Several modifications of the existing facility also appear to be required. These include:

1) Separate pillars sunk to bedrock on the North and East calibration coil axes. These will hold the two theodolites.
2) Two optically flat ports at right angles to each other in the thermal shroud to monitor changes in sensor orientation as a function of temperature.

One major problem likely to be encountered in the calibration procedures is digitizing the magnetometer output with sufficient precision. If a 16 bit Analog to Digital Converter is used for the +64K to -64K gamma dynamic range the least significant bit will correspond to 2 gamma. This uncertainty of $\pm$ 1 gamma limits the accuracy of the calibrations to an unacceptaboe level. Two solutions for this problem are possible:

1) Use a data logger to make a large number of samples and average to higher precision. (This works only if the facility noise is large.)
2) Use AC signals rather than DC signals as the calibration fields. If facility noise is low, small signals must be present in calibration axes orthogonal to main calibration fields. Use least square sine wave fits to determine AC signal amplitudes precisely.

Acknowledgements

We would like to thank Dr. H. Farthing of Goddard Space Flight Center and Mr. F. Mobley of the Johns Hopkins Applied Physics Laboratory for helpful comments on magnetometer calibration. Also, we thank Mr. E. Ieufer of Ames Research Laboratory and Mr. C.A. Harris of Goddard Space Flight Center for allowing us to visit their respective magnetometer calibration facilities. We are grateful to Dr. D. Jackson of UCLA for his suggestions concerning the solution of simultaneous nonlinear equations. One of us, Robert L. McPherron, would particularly like to thank Dr. D.J. Williams and the Space Environment Laboratory of NOAA in Boulder, Colorado for their hospitality and support while completing this work. This project has been supported by NASA Contract NAS 5-23660 as part of a design study for MAGSAT.

REFERENCES

Cain, J. C., Round table discussion of recommendations for revision of the IGRF. EOS, Trans. Amer. Geophy. Union; 56(8):538, 1975.

Harris, C. A., Supplement I (1971) to magnetic field restraints for spacecraft systems and subsystems. GSFC Rept. X-325-71-488, Dec. 1971.

Hildebrand, F. B., Introduction to Numerical Analysis. Mc-Graw-Hill, New York, 1956.

McLeod, M. G., Interim Report on a Proposed Triaxial Digital Fluxgate Magnetometer for NASA Application Explorer Mission--A Design Study. IGPP Pub. No. 1643, Oct. 1976.

McLeod, M. G. and J. D. Means, A Proposed Digital Fluxgate Magnetometer for NASA Applications Explorer Mission: Results of Tests of Critical Elements. IGPP Rept. No. 1698, May 1977.

Schneider, Eric J. and Thomas Kolany, The autocollimator. Optical Spectra: Fourth Qtr.:24-28, 1967.

Stern, D. P., Enhanced errors in models of the main geomagnetic field derived from scalar data. EOS, Trans. Amer. Geophy. Union, 56(8):547, 1975.

Yanagiliara, K., M. Kawamura, Y. Sano and T. Kuboki, New Standard Magnetic Observation System of Kakioka (KASMMER). Geophys. Magazine: 36(4):217-281, 1973.

Figure Captions

1. Schematic illustration showing the arrangement of calibration coils test table and theodolites. Theodolites and levels define the orthogonal, geographic coordinates $\hat{X}$, $\hat{Y}$, $\hat{Z}$. The direction cosines of the calibration coils in geographic coordinates are given by the non-orthogonal unit vectors $\hat{n}_X$, $\hat{n}_Y$, $\hat{n}_Z$.

2. Diagram showing a possible arrangement of three ring core sensors supported by a plastic cube and topped by a silvered, optical octagon. Normals to the faces of the octagon establish an orthogonal sensor coordinate system. The direction cosines of the magnetic axes of the ring cores in sensor coordinates are given by the non-orthogonal unit vectors $\hat{m}_X$, $\hat{m}_Y$, $\hat{m}_Z$.

3. A photograph of an earth inductor (or magnetic theodolite) showing the type of fixture required for calibrating the angular orientation of a sensor magnetic axis in sensor coordinates. As discussed in text the rotating search coil is replaced by a mounting plate to hold sensor.

4. A schematic diagram showing the modifications of the earth inductor required to obtain a magnetometer test fixture.

5. A schematic illustration showing how angles $\theta \sim 90^\circ$ and $\phi \approx 0^\circ$ are measured by theodolites to determine absolute orientation of normals to the faces of an optical octagon.

6. A fixture for aligning individual sensors with the calibration field.

7. Typical noise spectrum for a ring core fluxgate sensor. Horizontal brackets at top show frequency band measured by an experiment of given duration and sample rate. Dashed horizontal lines show quantization noise for $\delta B = 1\gamma$ and $\delta B \approx 1/32\gamma$.

8. Six relative orientations of sensor and coil used in first computer simulation.

9. Four relative orientations of sensor and coil necessary for a full calibration of three sensors and three coils.

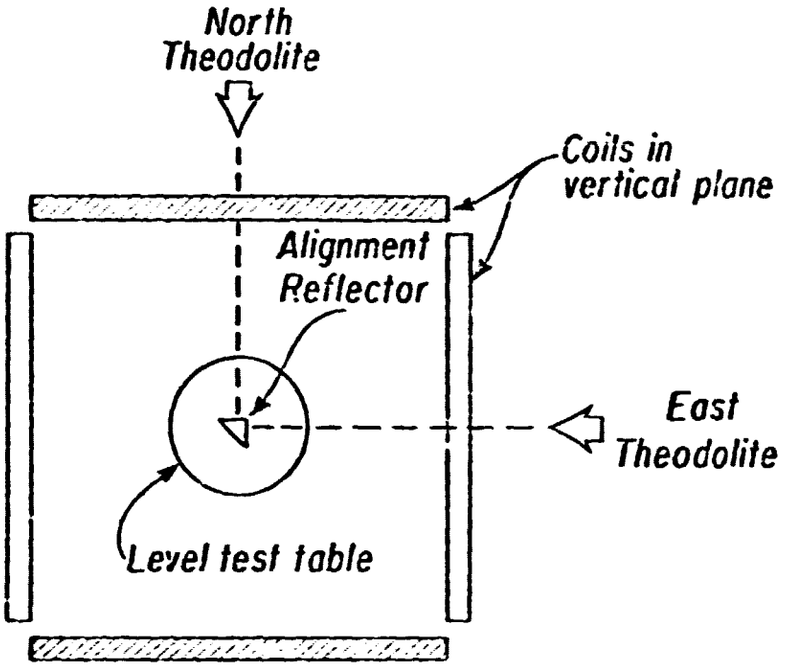
North
Theodolite
Coils in
vertical plane
Alignment
Reflector
East
Theodolite
Level test table

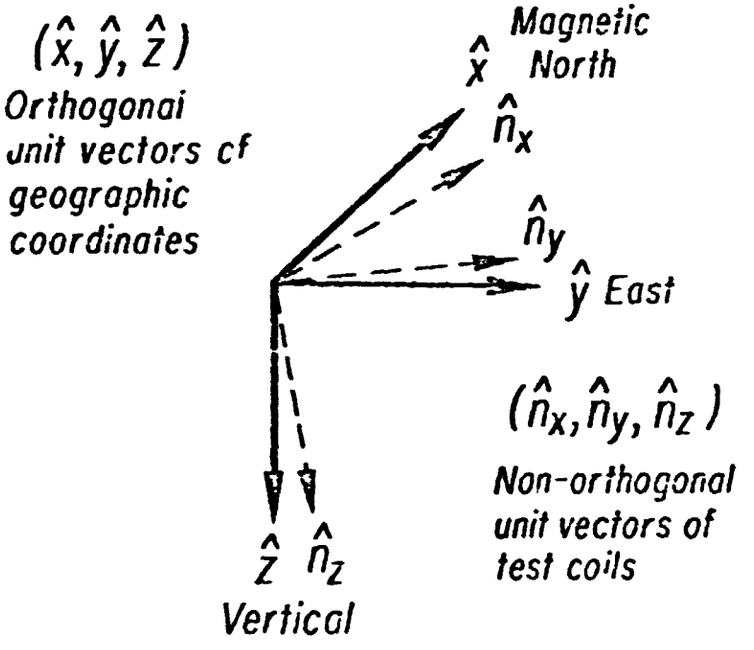
$(\hat{x}, \hat{y}, \hat{z})$
Orthogonal
unit vectors of
geographic
coordinates
$\hat{x}$ Magnetic
North
$\hat{n}_x$
$\hat{n}_y$
$\hat{y}$ East
$(\hat{n}_x, \hat{n}_y, \hat{n}_z)$
Non-orthogonal
unit vectors of
test coils
$\hat{z}$ $\hat{n}_z$
Vertical

Figure 1

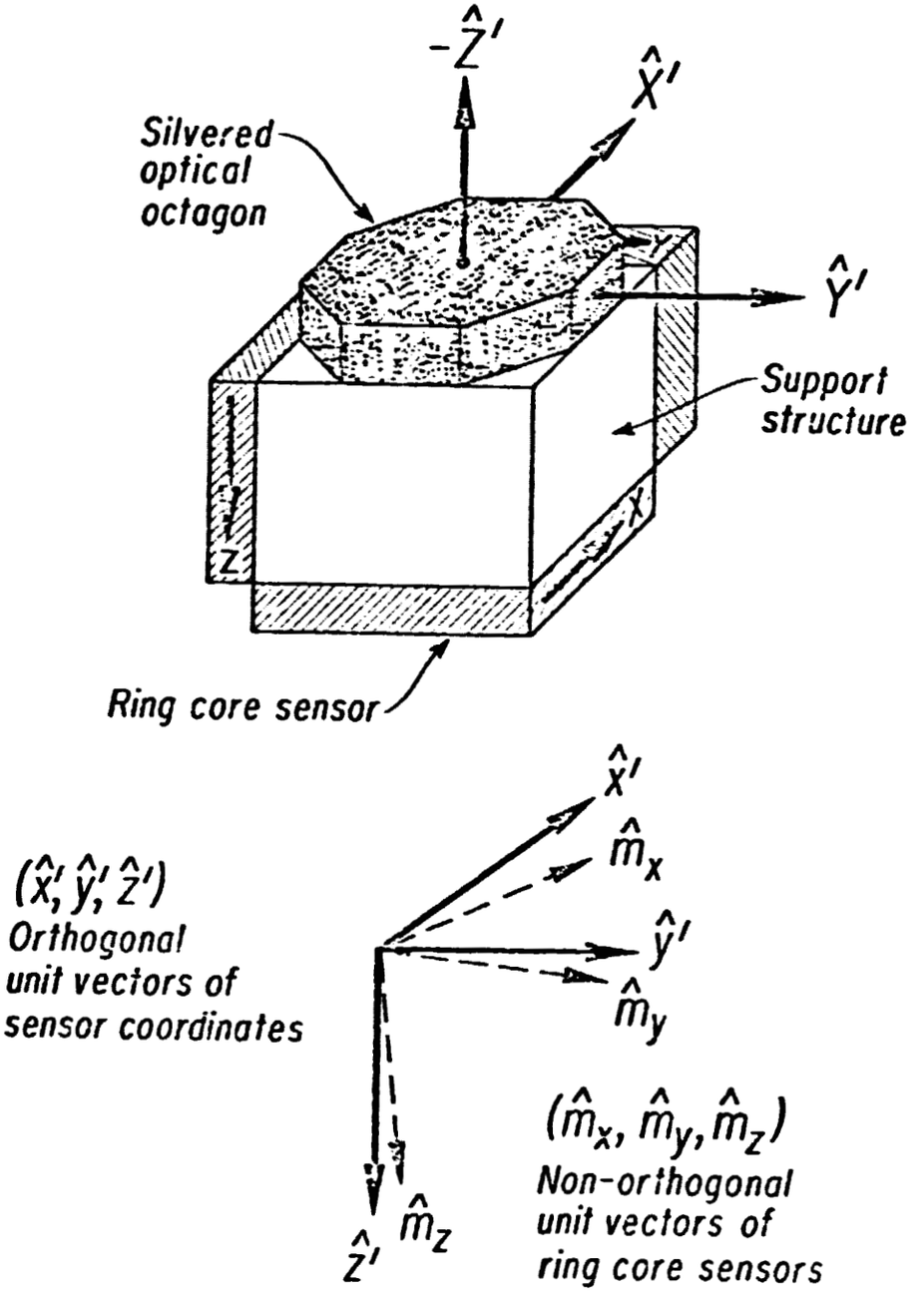
$-\hat{Z}'$
$\hat{X}'$
Silvered optical octagon
$\hat{Y}'$
Support structure
Z
X
Ring core sensor
$\hat{x}'$
$\hat{m}_x$
$\hat{y}'$
$\hat{m}_y$
$\hat{m}_z$
$\hat{z}'$
$(\hat{x}', \hat{y}', \hat{z}')$
Orthogonal unit vectors of sensor coordinates
$(\hat{m}_x, \hat{m}_y, \hat{m}_z)$
Non-orthogonal unit vectors of ring core sensors

Figure 2

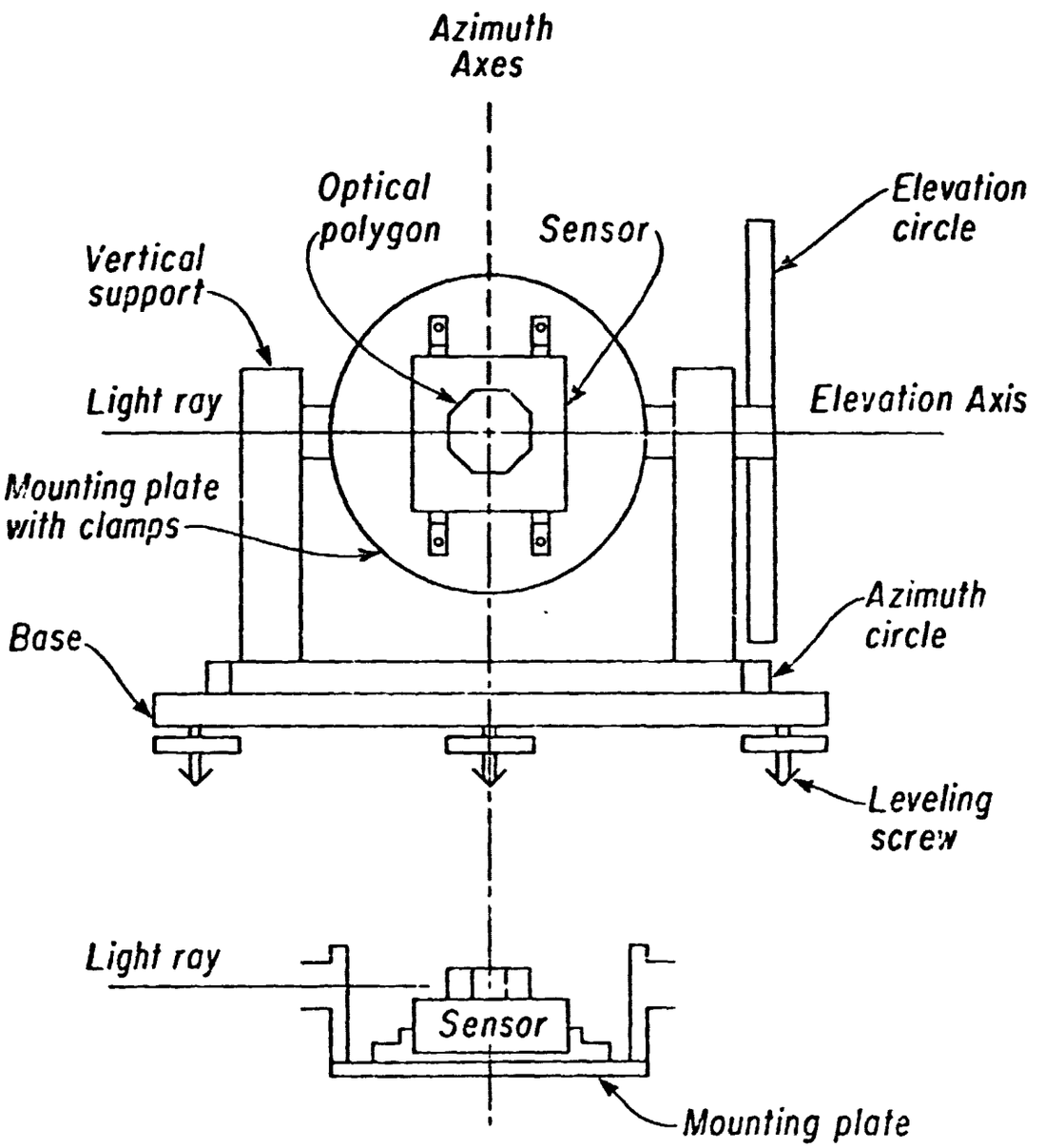
Azimuth
Axes
Optical
polygon
Sensor
Elevation
circle
Vertical
support
Light ray
Elevation Axis
Mounting plate
with clamps
Azimuth
circle
Base
Leveling
screw
Light ray
Sensor
Mounting plate

Figure 4

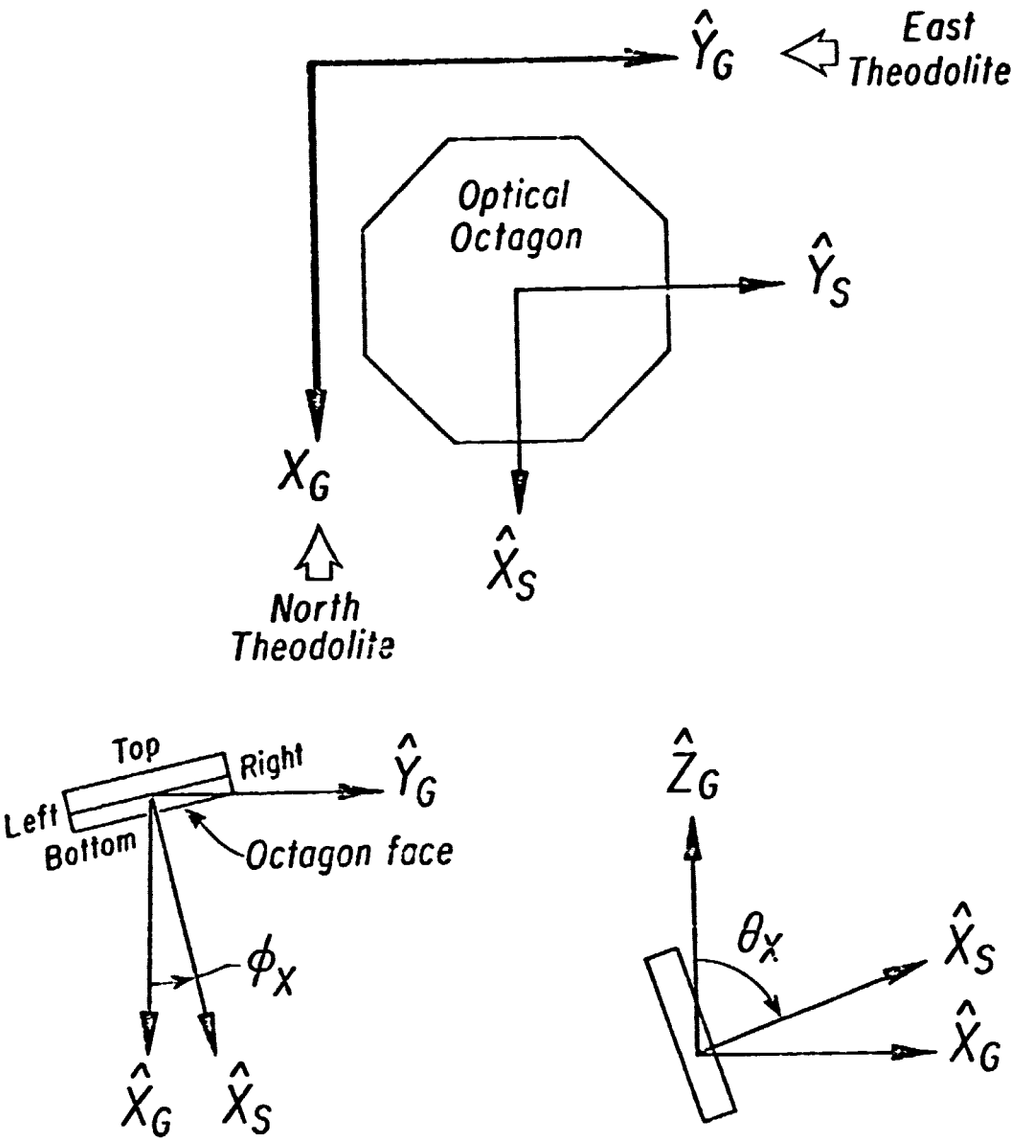
$\hat{Y}_G$
East
Theodolite
Optical
Octagon
$\hat{Y}_S$
X_G
$\hat{X}_S$
North
Theodolite
Top
Right
$\hat{Y}_G$
Left
Bottom
Octagon face
ϕ_X
$\hat{X}_G$
$\hat{X}_S$
$\hat{Z}_G$
θ_X
$\hat{X}_S$
$\hat{X}_G$

Figure 5.

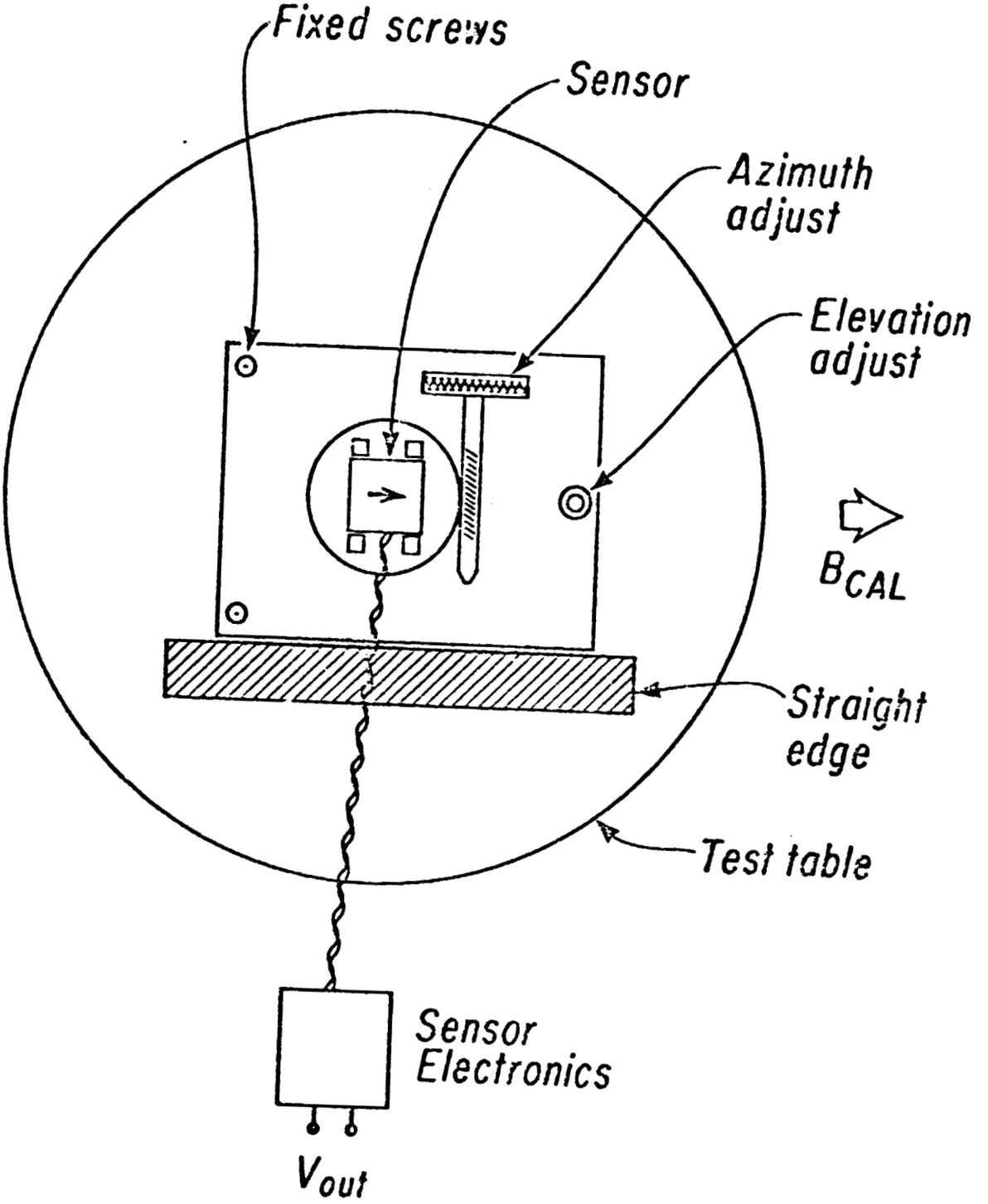
Fixed screws
Sensor
Azimuth adjust
Elevation adjust
B_{CAL}
Straight edge
Test table
Sensor Electronics
V_{out}

Figure 6

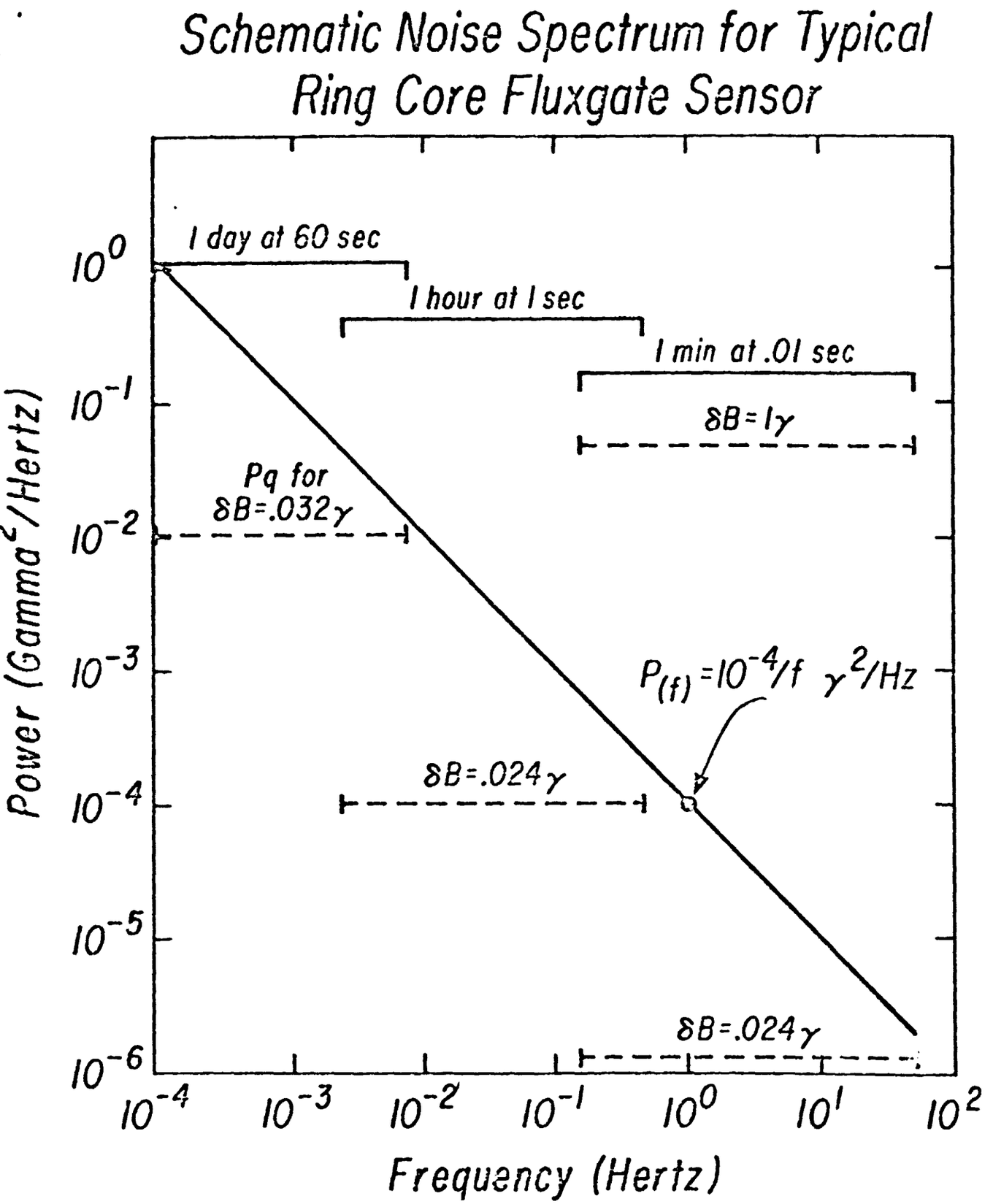
Schematic Noise Spectrum for Typical Ring Core Fluxgate Sensor
1 day at 60 sec
1 hour at 1 sec
1 min at .01 sec
δB=1γ
Pq for δB=.032γ
δB=.024γ
P(f)=10^-4/f γ^2/Hz
δB=.024γ
Power (Gamma^2/Hertz)
Frequency (Hertz)
10^0
10^-1
10^-2
10^-3
10^-4
10^-5
10^-6
10^-4
10^-3
10^-2
10^-1
10^0
10^1
10^2

Figure 7

Relative Orientations of Sensor and Geographic Coordinate Systems Used in First Computer Simulation

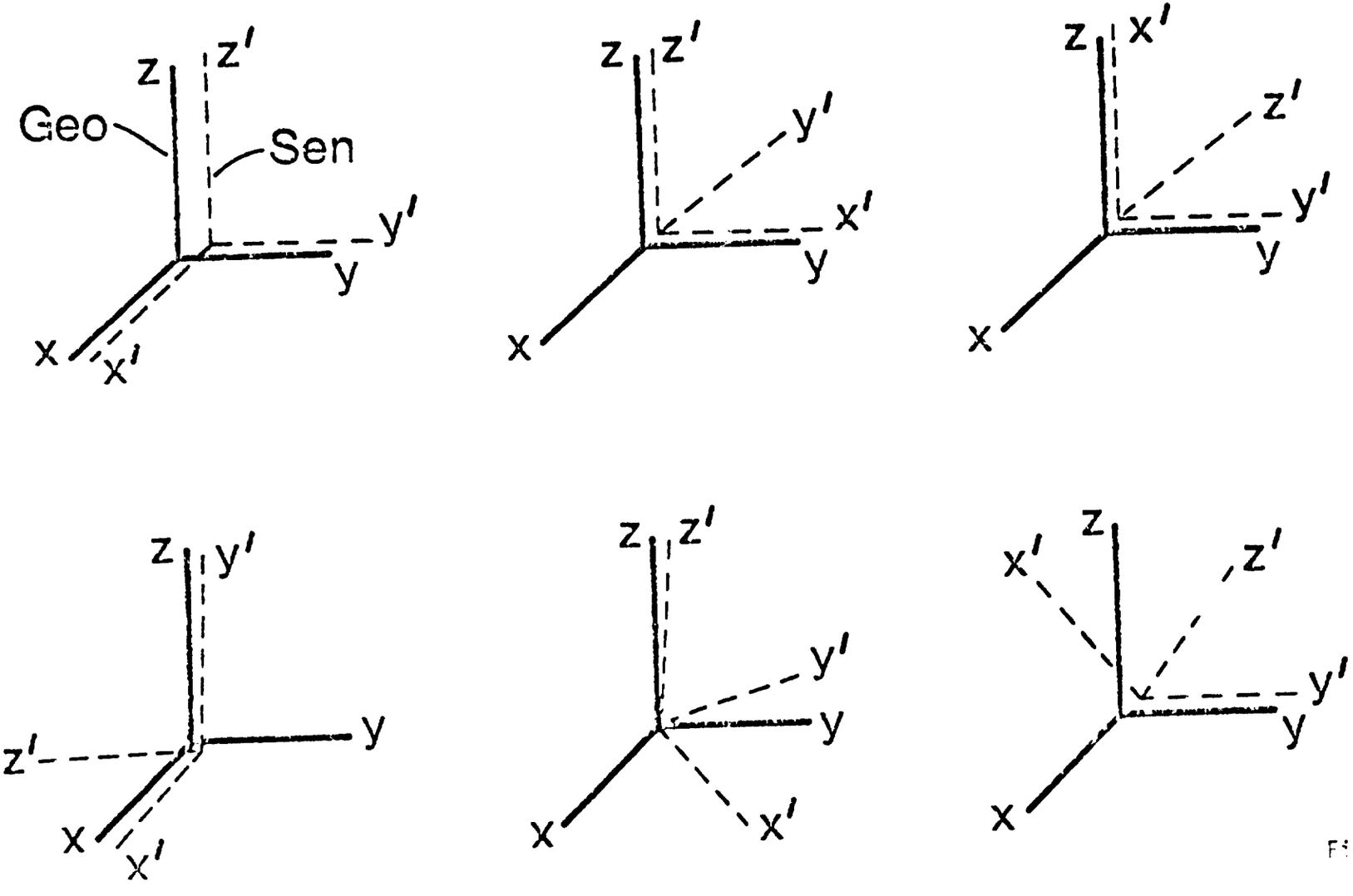

Figure 8

Relative Orientations of Sensors and Coils Necessary For Full Calibration

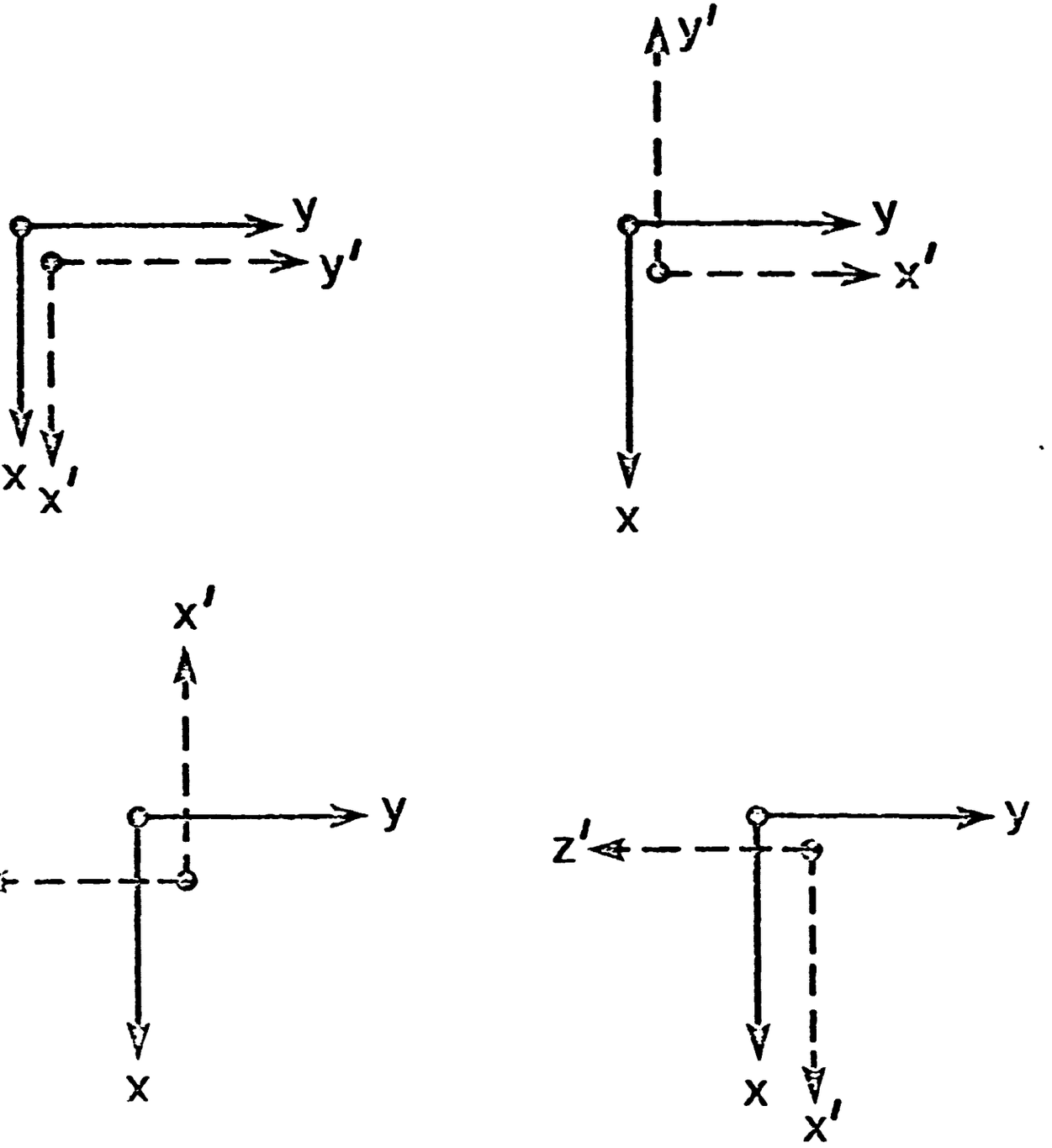

Figure 9

List of Tables

TABLE 1

TRANSFORMATIONS FOR SINGLE COIL-SINGLE SENSOR SIMULATION								
R1			R2			R3		
1.00000	.00000	.00000	.00000	1.00000	.00000	-1.00000	.00000	.00000
.00000	1.00000	.00000	-1.00000	.00000	.00000	.00000	-1.00000	.00000
.00000	.00000	1.00000	.00000	.00000	1.00000	.00000	.00000	1.00000

TRANSFORMATIONS FOR SINGLE COIL-SINGLE SENSOR SIMULATION								
R4			R5			R6		
1.00000	.00000	.00000	.70711	70711	.00000	.70711	.00000	.70711
.00000	.00000	1.00000	-.70711	.70711	.00000	.00000	1.00000	-.70711
.00000	-1.00000	00000	.00000	.00000	1.00000	.00000	.70711	.00000

TABLE 2

DIRECTION COSINES OF SENSOR AND COIL					
MU			NU		
.99975	.03	.05	.9983	-.01	.02
.01	.99875	.06	-.03	.99815	-.04
.02	.04	.99695	.05	.06	.999

TABLE 3

TRANSFORMATION MATRICIES USED IN SIMULATION

R1			R2			R3		
1.00000	00000	.00000	00000	1.00000	.00000	-1.00000	.00000	.00000
.00000	1.00000	.00000	-1.00000	00000	.00000	.00000	-1.00000	.00000
00000	.00000	1.00000	.00000	.00000	1.00000	.00000	.00000	1.00000

TRANSFORMATION MATRICIES USED IN SIMULATION

R4			R5			R6		
1.00000	.00000	.00000	.00000	.00000	1.00000	.00000	00000	1.00000
00000	.00000	1.00000	.00000	1.00000	.00000	.00000	-1.00000	.00000
.00000	-1.00000	.00000	-1.00000	.00000	.00000	1.00000	.00000	.00000

RMATION MATRICIES USED IN SIM

R7		
.00000	00000	1 00000
-1 00000	.00000	00000
.00000	-1.00000	.00000

TABLE 4

SIMULATED MEASUREMENTS FOR SEVEN ORIENTATIONS						
B	B	B	B	B	B	B
.998750	-.011550	-.994202	.030785	-.010780	.072289	
.001986	.999200	.000428	.999951	.027611	.040604	
.097962	.042332	.009385	.100818	.070253	-.994352	
.001104	.110324	.079310	.029721	.071394	-.027489	
.999002	-.020210	.997353	-.068394	.999555	.040122	
.119206	.018785	.999150	-.994555	.049803	-.028138	
.039575	.992753	.081036	.070166	-.995502	-.991506	
.000610	-.996750	.082823	.999102	-.066858	.999350	
.994553	.002014	-.029360	.072858	.999550	.011595	
-.038975	.001733	.019699	.997950	.070720	.088628	
-.995952	.001216	-.992006				

TABLE 5

COEFFECIENTS FOR THE EIGHTEEN UNKNOWNS											
RUN	I	J	DNX	DNY	DNZ	DNX	DNY	DNZ			
1	1	1	ROW 1			COL 1					
2	2	1	ROW 2				COL 1				
3	3	1	ROW 3					COL 1			
4	1	2		ROW 1		COL 2					
5	2	2		ROW 2			COL 2				
6	3	2		ROW 3				COL 2			
7	1	3			ROW 1	COL 3					
8	2	3			ROW 2		COL 3				
9	3	3			ROW 3			COL 3			
			$(\mu_0^T R)$			$(R\eta_0)$					

TABLE 6

MODIFICATIONS TO COEFFECIENTS OF UNKNOWNS

NUM	I	J	DNX	DNY	DNZ	DMX	DMY	DMZ
1	1	1	A11*V1			A110*V4		
2	2	1	A21*V1				A214*V5	
3	3	1	A31*V1					A318*V6
4	1	2		A45*V2		A410*V4		
5	2	2		A55*V2			A514*V5	
6	3	2		A65*V2				A618*V6
7	1	3			A79*V3	A710*V4		
8	2	3			A89*V3		A814*V5	
9	3	3			A99*V3			A918*V6
			$V1=\frac{\hat{n}_x^o}{n_{xx}^o}$	$V2=\frac{n_y^o}{n_{yy}^o}$	$V3=\frac{n_3^o}{n_{33}^o}$	$V4=\frac{\hat{m}_x^o}{m_{xx}^o}$	$V5=\frac{\hat{m}_y^o}{m_{yy}^o}$	$V6=\frac{\hat{m}_3^o}{m_{33}^o}$

List of Appendicies

A1. MAGSAT magnetometer specifications.

A2. SPEAKEZ program "MAGSIM" which generates simulated sensor output when excited by a calibration coil in a given orientation. Inputs are the direction cosines of the sensor and coil in their respective coordinate systems.

A3. SPEAKEZ program "MAGCAL 1" which solves for the direction cosines of sensor and coil using initial guess and simulated measurements.

A4. SPEAKEZ program "NEWSIM" which generates simulated measurements for three sensor and three coil simulation.

A5. SPEAKEZ programs "MAINPO," "EQUATS," and "SOLEQU." Together these programs use measurements of the transformation matrix and magnetometer output with an initial guess to solve for direction cosines of three sensors and three coils.

Appendix A1

MAGSAT magnetometer specifications.

Specifications for the Measurement of Vector Magnetic Fields

1. General - The magnetometer system described in this specification shall measure three orthogonal components of the ambient vector magnetic field aboard a low altitude earth-orbiting spacecraft. It is specifically intended for flight on the NASA Applications Explorer Mission (AEM) spacecraft. The spacecraft will be launched by a Scout vehicle into a near polar, low altitude orbit for the purpose of making a global survey of the earth vector magnetic field.

In order to minimize the effect of spacecraft magnetic fields, the sensor portion of the magnetometer will be mounted at the end of a 3-6 meter extensible boom to be provided by the spacecraft. Boom deflections and twist will be monitored by an attitude transfer system, provided by the spacecraft, which will make available an orthogonal transformation between the sensor coordinate system and the coordinate system of a stellar attitude determination system within the spacecraft body. If required for magnetic cleanliness, the electronics for the magnetometer can also be mounted within the spacecraft body, and connected to the magnetometer by cabling routed along the boom structure.

The magnetometer sensor shall have defined a geometric coordinate system, and means shall be provided through optically flat mirrors, or other optical devices, for determination of two orthogonal axes of the geometric coordinate system to one (1) arc second accuracy. The magnetometer shall measure projections of the ambient field along three orthogonal magnetic axes, whose nominal directions within the geometric coordinate system shall be specified to one (1) arc second precision.

2. Environmental Constraints - The environmental constraints on the magnetometer are presented in section 4 of this specification. All performance specifications of section 3 shall be met after exposure to shock, vibration and acceleration tests. All performance specifications shall be met under exposure to the orbital thermal and under ground simulation of that environment. It is expected that both active and passive thermal design of the magnetometer sensor will be necessary to satisfy the requirements of section 3.

3. Performance Specification

3.1 Stability of Magnetic Axes - The angular deviation of any magnetic axis from its nominal direction shall not exceed 5 arc seconds after exposure to shock, acceleration, and vibration testing in accordance with section 4 of this specification. The angular deviation of any magnetic axis from its nominal direction shall not exceed 5 arc seconds during exposure to the thermal-vacuum environment specified in section 4.

3.2 Orthogonality of Magnetic Axes - The angle between any two magnetic axes shall be 90° plus or minus 0.1°.

3.3 Range - The instrument shall be capable of measuring field components along any axis from -64000 gamma to plus 64000 gamma. (1 gamma equal to 10^{-9} Tesla).

3.4 Resolution - The resolution along any axis shall be plus or minus 1 gamma or less.

3.5 Measurement Bandwidth - The instrument shall be capable of measurement in a bandwidth of up to 25 Hz, and shall be compatible with bandwidth limiting to 1 Hz.

3.6 Noise - Fluctuation noise associated with any axis shall be less than 0.1 gamma zero-to-peak when measured for 10 seconds in a 25 Hz bandwidth.

3.7 Zero-Offset - The zero offset change associated with any axis shall be less than plus or minus 0.4 gamma over the expected range of sensor and electronics temperature. Long term stability of the zero offset shall be less than 0.4 gamma/year.

3.8 Absolute Accuracy - The total instrumental error from all sources in the determination of the field component along any sensor geometric axis shall be less than 5 gamma. This error budget includes the effects of magnetic axis stability, zero offset, fluctuation noise, quantization noise, sensitivity changes, and all other purely instrumental sources of error.

3.9 Power Consumption - The total power consumption for the magnetometer, including power for normal control of the sensor, shall be less than 6 watts.

3.10 Weight - Total weight of the system shall be less than 5 kilograms, inclusive of the boom cable interconnecting sensor and electronics.

3.11 Volume - The sensor structure shall be contained within a 30 cm. diameter sphere, while the electronics package shall be contained within a volume 20 cm x 15 cm x 15 cm.

4. Environmental Requirements

4.1 Vibration -

4.1.1 Sinusoidal Vibration:

Axis	Frequency Range (Hz)	Level (0 to Peak)	Sweep Rate (Oct/Min)
All (X,Y,Z)	10-18	5.0 g*	
	18-36	0.3 in (D.A.)	4.
	36-150	20.g	
	150-2500	5.g	

*Limited to 0.5 in double amplitude (D.A.)

4.1.2 Random Vibration

Axis	Frequency Range(Hz)	PSD Level (g^2/Hz)	Acceleration (g-rms)	Duration (minutes)
	20-200	0.045		
	200-400	+3dB/Oct	12.9	2/axis
	400-2000	0.090		

4.2 Acceleration - The performance specification of section 3 shall be satisfied after non-operating exposure of acceleration of 22.5G in the thrust axis and 6.0G in the lateral axis. The acceleration shall be simultaneously applied for a duration of three minutes.

4.3 Storage Temperature - Performance specifications shall not be compromised by non-operating storage for 6 hours at -50°C and 6 hours at plus 85°C.

4.4 Thermal Shock - The performance specifications shall not be compromised by exposure to 5 cycles of thermal shock, a cycle consisting of:

Step 1 - 1 hour storage at -50°C

Step 2 - transfer to plus 85°C in not more than 5 minutes

Step 3 - 1 hour storage at plus 85°C

Step 4 - transfer to -50°C in not more than 5 minutes

4.5 Electronics Operating Temperature - The performance specifications shall not be compromised by operation of the electronics at all temperatures in the range of -10°C to +50°C while the sensor is at room temperature conditions.

4.6 Thermal Vacuum Operation - The temperature of the sensor is to be actively and passively controlled by the contractor to insure temperatures compatible with the performance specifications of section 3. In orbit the sensor will be exposed to complete insolation and complete eclipse on a varying

duty cycle basis. The extremes of the cycling are expected to be (a) a continuous insolation for the indefinite period of time and (b) sixty (60) minutes of insolation to thirty (30) minutes of eclipse.

Confirmation of performance under these conditions will be performed by the government during acceptance tests of the magnetometer. The sensor will be operated at pressure of 1/2 micron or less in a non-magnetic thermal vacuum system and magnetic test facility in which the environment specified herein shall be simulated by use of a liquid nitrogen shroud and solar simulator. During these tests, the electronics will be operated at atmospheric pressure and in the temperature range -10°C to +50°C.

Appendix A2

```
tso logon rmp
ENTER TSO PASSWORD: ********
RMP LOGON IN PROGRESS AT 14:44:35 ON MAY 26, 1977
WELCOME TO UCLA-CCN TSO
READY: alloc fi(mykeep) da(mykeep)
READY: speakez
TSO SPEAKEASY 3 NU  2:45 PM MAY 26, 1977
:_libindex
A        BMEAS    CHECK    COMPAR   EQ       EQUATS   MACSOL   MAGCAL   MAGCAL1
MAGSIM   MAINPO   MMATRIX  MODEL    MUTNUT   N        NEWSECALNEWSIM   SENCAL
SENCAL1  SOLEQU   TMAT     TRAMAT
:_

edit magsim
MAGSIM  IS NOT DEFINED
MANUAL MODE
:_kept(magsim)
:_edit magsim
EDIT COMMAND MODE
:%

  1
EDITING MAGSIM
  1.0 PROGRAM
  2.0 INPUT MUYX,MUZX
  3.0 INPUT MUXZ,MUYZ
  4.0 MUXX=-1+SQRT(1-(MUYX**2+MUZX**2))
  4.1 MUZZ=-1+SQRT(1-(MUXZ**2+MUYZ**2))
  4.2 DELMU=VEC(:MUXX,MUYX,MUZX)
  4.3 DELMU=VEC(:MUXZ,MUYZ,MUZZ)
  4.4 XUV=VEC(:1 0 0)
  4.5 YUV=VEC(:0 1 0)
  4.6 ZUV=VEC(:0 0 1)
  4.7 MU=XUV+DELMU
  4.8 MU=ZUV+DELMU
  4.9 PRINT(DELMU,MU,DELMU,MU)
  5.0 R=MAT(3,3:)
  6.0 INPUT NE PLEASE
  7.0 PRINT(NE)
  8.0 M=VEC(12:)
  9.0 FOR I=1,NE
 10.0 PRINT ('DATA FOR EXPERIMENT #',I)
 11.0 INPUT R MATRIX PLEASE
 11.1 PRINT(R)
 12.0 MP=R*MU
 12.1 PRINT(MP)
 13.0 M(I)=INNER(MU,MP)
 13.1 PRINT(M)
*14.0 ENDLOOP I
:%
```

ORIGINAL PAGE IS
OF POOR QUALITY

2

C-1

Appendix A3

```
  kept(magcal1)
: edit magcal1
EDIT COMMAND MODE
:$list


pEDITING MAGCAL1
   1.00 PROGRAM
   1.10 MARGINS(132)
   1.20 INPUT NE THE NUMBER OF EXPERIMENTS
   1.30 AA=MAT(NE,4:)
   1.31 ME=VEC(NE:)
   1.50 CA=ME
   1.60 A=VEC(4:)
   2.00 PRINT('ARE OLD DATA AVAILABLE?')
   3.00 INPUT ANS (0=F& 1=T)
   4.00 IF(ANS.GE.1) GO TO LOC1
   9.00 FOR I=1,NE
  10.00 HENCEFORTH R IS OBJECT('R',I)
  11.00 PRINT('INPUT DATA FOR EXPERIMENT # ',I)
  12.00 INPUT ME(I) THE NORMALIZED MAGNETOMETER MEASUREMENT
  13.00 ME(I)
  15.00 INPUT R THE TRANSFORMATION MATRIX
  16.00 R
  17.00 ENDLOOP I
  18.00 INPUT RMSERR (THE RMS ERROR IN THE NORMALIZED MAGNETOMETER MEASUREMENTS
  19.00 VARYI=MAT(NE,1:)
  20.00 VARYI(,1)=RMSERR**2
  21.00 RMSERR;VARYI
  22.00 $
  22.50 INPUT MUY,MUZ (THE Y AND Z COMPONENT OF MU)
  24.00 INPUT NUX,NUY (THE X AND Y COMPONENTS OF NU)
  24.50 MUX=SQRT(1-MUY**2-MUZ**2)
  25.00 NUZ=SQRT(1-NUX**2-NUY**2)
  25.10 MU=VEC(:MUX,MUY,MUZ)
  25.20 NU=VEC(:NUX,NUY,NUZ)
  26.00 MU;NU
  28.00 LOC1:CONTINUE
  29.00 $
  30.00 FOR I=1,NE
  31.00 HENCEFORTH R IS OBJECT('R',I)
  32.00 CA(I)=INNER(MU,R*NU)
  33.00 A1=R*NU
  34.00 A2=TRANSPOSE(R)*MU
  34.50 A(1)=A1(2)-A1(1)*MUY/MUX
  35.00 A(2)=A1(3)-A1(1)*MUZ/MUX
  35.50 A(3)=A2(1)-A2(3)*NUX/NUZ
  36.00 A(4)=A2(2)-A2(3)*NUY/NUZ
  37.00 AA(I,)=A
  38.00 ENDLOOP I
  38.10 AA
  39.00 RES=ME-CA
  45.00 ME;CA;RES
  46.00 $
  47.00 SETNULL(1.0E-10)
  48.00 HENCEFORTH T IS TRANSPOSE
  49.00 $EIGENANALYSIS OF AA*T(AA)
```

```
 52.00 AUEV
 53.00 AUEVT=AUEV
 54.00 UP=U
 55.00 INPUT LOWLIM (LOWLIM IS THE LOWEST ACCEPTABLE EIGENVALUE)
 56.00 LOWLIM
 57.00 WHERE(AUEV.LT.(LOWLIM)) AUEVT=0
 58.00 IU=LOCS(AUEVT)
 59.00 IF(IU(1).EQ.1) GO TO LOCAU
 60.00 I=LOCS(.NOT.AUEVT)
 61.00 UP=U(,IU)
 62.00 UO=U(,I)
 63.00 LOCAU:CONTINUE
 64.00 $EIGENANALYSIS OF T(AA)*AA
 65.00 AV=T(AA)*AA
 66.00 AVEV=EIGENVALS(AV,V)
 67.00 AVEV
 68.00 AVEVT=AVEV
 69.00 VP=V
 70.00 WHERE(AVEV.LT.LOWLIM) AVEVT=0
 71.00 IV=LOCS(AVEVT)
 72.00 IF(IV(1).EQ.1) GO TO LOCAV
 73.00 I=LOCS(.NOT.AVEVT)
 74.00 VP=V(,IV)
 75.00 VO=V(,I)
 76.00 LOCAV:CONTINUE
 77.00 $SEE IF UP AND VP GIVE A POS DEF DIAG MAT
 78.00 L=T(UP)*AA*VP
 79.00 DE=DIAGELS(L)
 80.00 WHERE(DE.GT.0) DE=0
 81.00 IFX=LOCS(DE)
 82.00 $CHANGE SIGN OF COLUMNS OF UP CORRESPONDING TO NEGATIVE EIGENVALUES
 83.00 NDO=NOELS(IFX)
 84.00 IF(IFX(1).EQ.0) GO TO BELOW
 85.00 FOR I=1,NDO
 86.00 UP(,IFX(I))=-UP(,IFX(I))
 87.00 ENDLOOP  I
 88.00 BELOW:CONTINUE
 89.00 L=T(UP)*AA*VP
 90.00 DIAGELS(L)
 91.00 INVAA=VP*(1/L)*T(UP)
 92.00 X=INVAA*RES
 93.00 NR=NOROWS(INVAA)
 94.00 NC=NOCOLS(INVAA)
 94.10 H2=MAT(NR,NC:)
 95.00 FOR I=1,NR
 96.00 FOR J=1,NC
 97.00 H2(I,J)=INVAA(I,J)**2
 98.00 ENDLOOP J
 99.00 ENDLOOP I
100.00 VARXK=H2*VARYI
101.00 SQRT(VARXK)
101.10 IF(IU(1).EQ.1) GO TO HERE
102.00 VAR=(T(UO)*RES)**2
103.00 LRESSQ=RES**2
104.00 VAR;LRESSQ;VAR/LRESSQ
104.10 HERE:CONTINUE
105.00 X
106.00 MUY=X(1)+MUY
106.50 MUZ=X(2)+MUZ
107.00 MUX=X(3)+MUX
107.50 MUY=X(4)+MUY
108.00 MUX=SQRT(1-MUY**2-MUZ**2)
108.50 MUZ=SQRT(1-MUX**2-MUY**2)
109.00 MU=VEC(:MUX,MUY,MUZ)
```

```
 113.00 NU;NU**2
 114.00 PRINT('ARE THESE VALUES GOOD ENOUGH?')
 115.00 INPUT ANS (0=F & 1=T)
 116.00 IF(ANS) GO TO PROEND
 117.00 GO TO LOC1
 118.00 PROEND:CONTINUE
 119.00 AA;INVAA;U;V;INVAA*AA;AA*INVAA;H2
 119.10 IF(IU(1).NE.1) PRINT(VO,UO,T(UO)*RES)
*120.00 PRINT('NORMAL END OF PROGRAM NAGCAL')
:%

  end
p


enter apl or tso

tso

360/91 temporarily not available

6
```

Appendix A4

```
  end
MANUAL MODE
: edit newsim
NEWSIM  IS NOT DEFINED
MANUAL MODE
:_kept(newsim)
: edit newsim
EDIT COMMAND MODE
:$


  1
EDITING NEWSIM
  1.0 PROGRAM
  2.0 INPUT MUT A MAT WITH ROWS BEING UNIT VEC OF SEN IN SEN COOR
  3.0 INPUT NUT A MAT WITH ROWS BEING UNIT VEC OF COIL IN GEO COOR
  4.0 HENCEFORTH T IS TRANSP
  5.0 MU=T(MUT);NU=T(NUT)
  6.0 MU;NU
  7.0 $OBTAIN LIST DEFINING NUM OF SEN ORIENT AND TRANS MAT
  8.0 KEPTLIST(TMAT)
  9.0 ROWS=9*NE
 10.0 B=VEC(ROWS:)
 11.0 $
 12.0 $LOOP TO CREATE MEASUREMENT MAT FOR CAL MAT BC=I
 13.0 L=1
 14.0 FOR K=1,NE
 14.1 PRINT ('EXPERIMENT # =', K)
 15.0 HENCEFORTH R IS OBJECT('R',K)
 16.0 BM=MUT*R*NU;BM
 17.0 $
 18.0 $ PUT COLUMNS OF BM INTO COLUMN VEC OF MEASUREMENTS
 19.0 FOR J=1,3
 20.0 B(L)=BM(,J)
 21.0 L=L+3
 22.0 ENDLOOP J;ENDLOOP K
 23.0 $PRINT AND SAVE THIS VECTOR
 24.0 TMAT=NAMELIST(NE,R1,R2 R3 R4 R5 R6,R7 ,B)
 25.0 KEEPLIST(TMAT)
*26.0 B
:$


  end
MANUAL MODE
:_
```

Appendix A5

```
EDITING MAINPO
  1 PROGRAM
  2 $ FROM HERE TO ITLOOP: IS PROGRAM INITIALIZATION
  3 DELNU=MAT(3,3:);DELNU=DELMU
  4 PRINT('INITIALIZE PROGRAM TO CALCULATE SENSOR AND COIL COSINES')
  5 INPUT MUT,NUT (ROWS ARE GUESSES OF SENSOR AND COIL UNIT VECTORS)
  6 HENCEFORTH T IS TRANSPOSE
  7 MU=T(MUT);NU=T(NUT)
  8 PRINT('THE INITIAL MODEL ON INPUT WAS')
  9 MU;NU
 10 $
 11 $ OBTAIN MEASURED TRANSFORMATION MATRICIES
 12 RR=MAT(21,3:)
 13 KEPT(TRAMAT)
 14 LOADDATA(RR,TRAMAT)
 15 PRINT('THE INPUT TRANSFORMATION MATRICIES ARE')
 16 RR
 17 $
 18 $ OBATAIN MEASURED FIELD VALUES
 19 KEPTLIST(BMEAS)
 20 B
 21 $
 22 $ FREE AS MUCH SPACE AS POSSIBLE
 23 FREE(MUT,NUT,TRAMAT)
 24 $
 25 $ FIND OUT HOW MANY SENSOR ORIENTATIONS MEASURED
 26 INPUT NE (THE NUMBER OF SENSOR ORIENTATIONS)
 27 ROWS=9*NE
 28 $
 29 $ COME HERE FOR ITERATION OF SOLUTION
 30 LSTOP=3
 31 LMP=1
 32 ITLO  :
 33 $ OBTAIN AN EXECUTE PROGRAM TO CREATE EQUATIONS FOR THIS MODEL
 34 PRINT('BEGINNING ITERATION NUMBER ',LMP)
 35 KEPT(EQUATS)
 36 EXECUTE(EQUATS)
 37 FREE(EQUATS)
 38 $ OBTAIN AND EXECUTE PROGRAM TOS SOLVE EQUATIONS
 39 $KEPT(SOLEQU)
 40 $EXECUTE(SOLEQU)
 41 $FREE(SOLEQU)
 42 KEPT MACSOL
 43 EXECUTE MACSOL
 44 FREE MACSOL
 45 LMP=LMP+1
 46 IF(LMP.LE.LSTOP) GO TO ITLOOP
 47 MU=MU+DELMU;NU=NU+DELNU
 48 DELMU;DELNU;MU;NU
 49 PRINT('INITIAL MODEL HAS BEEN IMPROVED LSTOP TIMES',LSTOP)
```

```
  edit equats
EDIT COMMAND MODE
:$
```

```
  list
EDITING EQUATS
  1 PROGRAM EQUATS
  2 $ UPDATE MU AND NU WITH PREVIOUSLY CALCULATED CORRECTIONS
  3 MU=MU+DELMU;NU=NU+DELNU
  4 DELMU;DELNU
  5 FREE(DELMU,DELNU)
  6 $ CALCULATE DIAGONAL ELEMENTS OF MU AND NU USING OFF DIAG ELE
  7 MU(1,1)=SQRT(1-MU(2,1)**2-MU(3,1)**2)
  8 NU(1,1)=SQRT(1-NU(2,1)**2-NU(3,1)**2)
  9 MU(2,2)=SQRT(1-MU(1,2)**2-MU(3,2)**2)
 10 NU(2,2)=SQRT(1-NU(1,2)**2-NU(3,2)**2)
 11 MU(3,3)=SQRT(1-MU(1,3)**2-MU(2,3)**2)
 12 NU(3,3)=SQRT(1-NU(1,3)**2-NU(2,3)**2)
 13 PRINT('MU AND NU AS CORRECTED TO GIVE UNIT COL NORMALS ARE')
 14 MU;NU
 15 $CREATE UNIT VECTOR CONSTRAINT MATRIX
 16 V1=NU(,1)/NU(1,1)
 17 V2=NU(,2)/NU(2,2)
 18 V3=NU(,3)/NU(3,3)
 19 V4=MU(,1)/MU(1,1)
 20 V5=MU(,2)/MU(2,2)
 21 V6=MU(,3)/MU(3,3)
 22 $DO LOOP FOR EACH ORIENTATION
 23 PRINT('BEGINNING LOOP FOR EACH SET OF SENSOR ORIENTATIONS')
 24 J= 1 5 9 10 14 18
 25 L=1
 26 A=MAT(ROWS,12:);BR=VEC(ROWS:)
 27 FOR K=1,NE
 28 AA=MAT(9,18:);NN=MAT(9,18:);RNX=MAT(7,3:);BMOD=VEC(9:)
 29 RNX=MAT(7,3:)
 30 $ PUT PROPER TRANSFORMATION MATRIX IN R
 31 IT=3*(K-1)+1
 32 ISA=IT,IT+1,IT+2
 33 R=RR(ISA,)
 34 $CALCULATE MODEL MATRICIES
 35 C1=T(MU)*R;C2=R*NU;BMM=T(MU)*R*NU
 36 RNX(1)=C2(,1)
 37 RNX(4)=C2(,2)
 38 RNX(7)=C2(,3)
 39 $ SET UP MODEL MEASUREMENT VECTOR
 40 BMOD(1)=BMM(,1)
 41 BMOD(4)=BMM(,2)
 42 BMOD(7)=BMM(,3)
 43 ISA=INTEGERS(L,L+8)
 44 BB=B(ISA)
 45 BR(L)=BB-BMOD
 46 $SET UP LEFT HALF OF COEFFECIENT MATRIX
 47 AA(1,1)=C1
 48 AA(4,4)=C1
 49 AA(7,7)=C1
 50 $SET UP RIGHT HALF OF COEFFECIENT MAATRIX
 51 AA(1,10)=RNX
 52 AA(2,13)=RNX
 53 AA(3,16)=RNX
 54 NN(1,1)=COLARRAY(9:AA(,1))*ROWARRAY(3:V1)
 55 NN(1,4)=COLARRAY(9:AA(,5))*ROWARRAY(3:V2)
 56 NN(1,7)=COLARRAY(9:AA(,9))*ROWARRAY(3:V3)
 57 NN(1,10)=COLARRAY(9:AA(,10))*ROWARRAY(3:V4)
```

```
 59 NN(1,15)=COLARRAY(9:AA(,16))*ROWARRAY(3:V6)
 60 AA=AA-MFAM(NN)
 61 AA=ELIMCOLS(AA,J)
 62 A(L,1)=AA
 63 L=L+9
 64 ENDLOOP K
 65 BR
 66 FREE(V1,V2,V3,V4,V5,V6,J,K,AA,NN,IT,ISA,R,C1,C2,BMM,RNX,BMOD,BB)
*67 PRINT('PROGRAM EQUATS HAS COMPLETED CALCULATION OF EQUATIONS FOR THIS MODE
:$
```

```
  end
MANUAL MODE
:_keep(solequ)
:_edit solequ
EDIT COMMAND MODE
:%list


EDITING SOLEQU.
   1 PROGRAM
   2 $ INITIALIZE ARRAYS FOR SOLVING SET OF EQUATIONS
   3 X=VEC(ROWS:)
   4 T=1.0E-6
   5 S=ARRAY(12:)
   6 X=SIMEQUAT(A,BR,T:S)
   7 $
   8 $ SET UP CORRECTION MATRICIES
   9 DELNU=TRANSP(MAT(3,3:0 X(1) X(2) X(3) 0 X(4) X(5) X(6) 0 ))
  10 DELNU=TRANSP(MAT(3,3:0 X(7) X(8) X(9) 0 X(10) X(11) X(12) 0 ))
  11 FREE(X,T,S,A,BR)
  12 $
*13 PRINT('PROGRAM SOLEQU HAS COMPLETED SOLUTION OF EQUATIONS FOR THIS MODEL')
:%
```